N73-12392

MSC-07293

NASA TECHNICAL MEMORANDUM

NASA TM X-58099
November 1972

CASE FILE COPY

EFFECTS OF BURIED OBSTACLES ON PENETRATION RESISTANCE IN COHESIONLESS SOILS

NATIONAL AERONAUTICS AND SPACE ADMINISTRATION
MANNED SPACECRAFT CENTER
HOUSTON, TEXAS 77058

1. Report No. NASA TM X-58099	2. Government Accession No.	3. Recipient's Catalog No.
4. Title and Subtitle EFFECTS OF BURIED OBSTACLES ON PENETRATION RESISTANCE IN COHESIONLESS SOILS		5. Report Date November 1972
		6. Performing Organization Code
7. Author(s) Ernest W. DeLuca, MSC, and Lisimaco H. Carrasco, Lockheed Electronics Company		8. Performing Organization Report No. MSC-07293
9. Performing Organization Name and Address Manned Spacecraft Center Houston, Texas 77058		10. Work Unit No. 914-50-15-06-72
		11. Contract or Grant No.
12. Sponsoring Agency Name and Address National Aeronautics and Space Administration Washington, D.C. 20546		13. Type of Report and Period Covered Technical Memorandum
		14. Sponsoring Agency Code

15. Supplementary Notes

16. Abstract

Studies of penetration resistance in cohesionless soils with respect to the soil physical properties of relative density, texture, and gradation have been conducted in the past without regard to the presence of buried solid obstacles. This document presents recent experiments concerning penetration of cohesionless soils in special molds that include solid obstacles embedded within the soil matrix. The relative effects of these obstacles with respect to the soil parameters just mentioned also are discussed. Because lunar soil is fairly cohesionless, special attention has been given to the Apollo Lunar Simulant, AP-12. Extensive use has been made of results obtained from reports generated by and for NASA and other Government and private agencies.

17. Key Words (Suggested by Author(s)) · Penetration Profile · Relative Density · Texture · Gradation · Penetrometer	18. Distribution Statement

19. Security Classif. (of this report) None	20. Security Classif. (of this page) None	21. No. of Pages 74	22. Price

NASA — MSC

NASA TM X-58099

EFFECTS OF BURIED OBSTACLES ON PENETRATION RESISTANCE IN COHESIONLESS SOILS

Ernest W. DeLuca
Manned Spacecraft Center
Houston, Texas 77058

and

Lisimaco H. Carrasco
Lockheed Electronics Company
Houston, Texas 77058

CONTENTS

TABLES

FIGURES

Figure Page

EFFECTS OF BURIED OBSTACLES ON PENETRATION RESISTANCE IN COHESIONLESS SOILS

By Ernest W. DeLuca and Lisimaco H. Carrasco*
Manned Spacecraft Center

SUMMARY

A study was made of the effects of buried solid obstacles on penetration resistance in cohesionless soils. Resulting profiles were compared with original penetration profiles of the same soils containing no obstacles.

It was found that the effect of obstacles on penetration resistance was a function of relative density and average grain size but was not strongly influenced by gradation (grain-size distribution) within the range tested (uniformity coefficient = 1.90 to 6.17). The effects of varying depth and size of the obstacles themselves also were found to be significant.

The separate effects again were analyzed in terms of work required to overcome obstacle resistance in order to provide a meaningful interrelationship between the parameters being studied. Recommendations for further study involving penetrometer size and shape, layers of different soil densities, and interference levels (center-to-center distance between the penetrometer and an obstacle) were made.

INTRODUCTION

Past studies conducted on penetration resistance in cohesionless soils have established definite relationships between this resistance and several physical parameters. The most significant parameters, with respect to soil type, are relative density, texture (average grain size), and gradation (grain-size distribution) (ref. 1). With respect to penetrometers, the most significant parameters are the size and shape of the penetrating head and the depth of penetration.

To date, with the exception of rather limited research on soil stratification (that is, layers of different densities), knowledge concerning the nature of solid obstacles within the penetration influence area of a soil matrix and the effect of these obstacles on penetration resistance is practically nonexistent. The penetration influence area is that portion of the pressure zone formed by the penetrometer head that is directly above the projected area of the obstacle. The penetration influence area is illustrated in figure 1.

---

*Lockheed Electronics Company.

Penetration resistance profiles for particular soils may be determined experimentally through laboratory procedures. If the parameters mentioned previously are held constant or are varied in a predictable manner, penetration profiles may be obtained with different patterns of buried obstacles added to the soil matrix. Then, these resulting profiles can be compared readily with the originally established profiles of the same soil type. Thus, the problem to be studied is three-fold in nature and is defined as follows.

1. Establish original penetration resistance profiles for a particular soil type without obstacles and with all known parameters held constant

2. For this same soil type, establish penetration resistance profiles with all known parameters varied in a predictable manner and with known patterns of buried solid obstacles added to the soil matrix

3. Compare the obstacle penetration resistance profiles with the original penetration resistance profiles

This study was prepared for the NASA Manned Spacecraft Center at Houston, Texas. Experimental analysis was conducted in the laboratories of Lockheed Electronics Company, Houston Aerospace Systems Division, under direct supervision and technical guidance of W. David Carrier, III. The report was compiled with the assistance of Ralf Schmidt.

SYMBOLS

A_o	obstacle area
C_u	coefficient of uniformity
D_B	diameter of container base
D_o	diameter of obstacle
D_r	relative density of soil
D_s	average grain size (diameter) of soil
F	vertically applied force, f(z)
F_m	maximum vertical force
G_s	grain-size distribution (gradation) of soil
H	height of displacement

H_c	inner height (depth) of container
H_o	obstacle height
H_T	total height of container
ID	inside diameter
OD	outside diameter
P_m	maximum pressure, F_m/A_o
V	displacement volume
V_o	obstacle volume
W_r	work necessary to overcome obstacle resistance
Z	displacement depth
Z_o	depth of obstacle
α	displacement angle
γ	unit weight at which soil has been placed
γ_{max}	maximum unit weight at which soil can be placed
γ_{min}	minimum unit weight at which soil can be placed
γ_o	obstacle density
ϕ	circular

PURPOSE OF STUDY

This study forms a supplement to a previous document on the Soil Penetration Resistance Study (SPERS) Program (ref. 2). The ultimate goal of SPERS is to utilize penetration resistance profiles provided by Apollo 15 and other subsequent missions and to predict, with fair accuracy, the nature of the lunar subsurface with respect to relative density; stratification (change in density with depth); and most significantly, the existence, depth, and relative size of buried obstacles.

Evidence obtained from previous Apollo missions (ref. 3) substantiates earlier findings of Surveyors I, III, V, VI, and VII that lunar soil is fairly cohesionless. With respect to this determination, the primary objectives of this study are as follows.

1. To establish original penetration resistance profiles for several cohesionless soils without obstacles, at least one of which is a lunar simulant

2. To establish penetration resistance profiles of each soil with various patterns of buried obstacles

3. To explore the relative effects of buried obstacles, with respect to penetration resistance, by comparison of obstacle interference patterns (that is, penetration profiles obtained with buried obstacles) with the original penetration profiles

ESTABLISHMENT OF CRITERIA FOR ANALYSIS

The parameters influencing penetration resistance of a cohesionless soil and their corresponding ranges of variation are discussed separately.

Soil Properties

The relative density of a soil is proportional to its bulk density according to the relationship (ref. 4)

$$D_r = \frac{\gamma_{max}}{\gamma} \times \frac{\gamma - \gamma_{min}}{\gamma_{max} - \gamma_{min}} \times 100 \text{ percent} \qquad (1)$$

where D_r = relative density (percent)

γ_{max} = maximum unit weight at which the soil can be placed

γ_{min} = minimum unit weight at which the soil can be placed

γ = unit weight at which the soil has been placed

Values for γ_{max} and γ_{min} and the resulting relative density equations for the soils analyzed are summarized in table I. Because penetration resistance also varies directly with bulk density, the logical decision was to analyze each soil within as inclusive a range of relative densities as possible.

Texture refers to coarseness or fineness of a soil and is reflected in the average grain size. It was determined that a minimum of three cohesionless soils be analyzed to include this effect.

To eliminate possible variation of penetration resistance values caused by differences in gradation, soils were selected with approximately the same uniformity coefficient (C_u). The uniformity coefficient of a soil is defined as the ratio of D_{60} to D_{10}, where D_{60} is the soil-particle diameter of which 60 percent of the soil is finer and D_{10} is the corresponding value at 10 percent finer (ref. 5). The exception was the Apollo Lunar Simulant AP-12, which was eventually used as control soil for analysis of grain-size distribution effects. Information on grain-size-distribution curves is included in appendix A.

Lunar soils contain no moisture or free water. To be considered negligible, moisture contents of all soils were reduced to air dry (<0.1 percent).

Experimental Apparatus

Penetrometers are classified as either cone type or plate type. For a cone penetrometer, the projected area at the base of the head is used in determining bearing capacity of a soil; whereas, that used for a plate is the actual contact area. For the present preliminary investigations, a cone penetrometer was selected.

Soil is subject to creep under load. Establishment of a standard rate of penetration was necessary to minimize creep and plastic deformation.

The size of mold in which soils investigations are conducted is significant, as determined through research by the United States Army Corps of Engineers Waterways Experiment Station in Vicksburg, Mississippi (ref. 6). Their study revealed that the average mold size should be greater than 20.32 centimeters (8 inches) in diameter to avoid any secondary effects contributed by the mold walls. Shape has little effect as long as this mean diameter is maintained. The sample used to establish penetration profiles should be of sufficient depth to allow the penetrometer to travel its entire length and avoid "bottoming out" on the base of the mold; 15.24 centimeters (6 inches) beyond the overall length of the penetrometer was considered sufficient.

Effect of Obstacles

It has been proposed (ref. 2) that the solid volume occupied by buried obstacles is critical within the penetration influence area. A size range of obstacles including small, medium, and large was considered adequate for analysis of this particular effect. Geometry was not considered as a parameter for preliminary investigation.

Penetration resistance increases with depth in a homogeneous, cohesionless soil. Thus, it was reasonable to assume that obstacles located at various depths along the path of the penetrometer axis would affect the resistance profile significantly. A suitable range selected for analysis of depth effect was 15.24, 30.48, and 45.72 centimeters (6, 12, and 18 inches).

An interference level is defined as the perpendicular distance between the penetrometer axis and center of mass of an obstacle (ref. 2). Interference levels greater than zero were not considered in this study.

SELECTION OF FINAL PARAMETERS

Parameters were selected on the basis of the criteria mentioned previously. The parameters are summarized in the following sections.

Soil Types

Four homogeneous, cohesionless soils were selected on the basis of texture and gradation. Grain-size-distribution curves for these soils are found in appendix B. The four soils were the following.

1. Bendix Medium Sand (MS)

2. Standard Ottawa Sand (OS)

3. League City Sand (LCS)

4. Apollo Lunar Simulant (AP-12)

Bendix Medium Sand is a coarse-grained soil of uniform gradation (developed by the Bendix Corporation) that represents the upper range of grain sizes analyzed. Ottawa Sand is also uniformly graded and represents the medium range of grain sizes analyzed. League City Sand is a uniform, cohesionless soil found in the vicinity of League City, Texas, and is representative of the lower grain-size range. The AP-12 is a well-graded mixture of cohesionless ground basalt that was prepared with the same average grain-size distribution as the samples retrieved from the Apollo 12 mission for use as a lunar simulant.

Ranges of relative density D_r used in the development of standard penetration resistance curves for each soil are shown in table II. All soils were analyzed at a moisture content of less than 0.1 percent. Individual values ranged as shown in table III.

Laboratory Equipment

A standard 30° cone penetrometer with base area of 0.50 square inches (3.22 sq cm) was selected for penetration studies. The cone is a product of the U.S. Army Corps of Engineers and was developed by the Waterways Experiment Station (WES). The total travel of the penetrometer stem is 870.25 centimeters (29.50 inches) from base of cone to underside of collar flange. A diagram of the penetrometer system is shown in figure 2. Photographs of the separate components may also be found in figures C-1, C-2, and C-4 of appendix C. The standard rate of penetration for the 30° cone penetrometer described has been established at 182.88 cm/min (72 in/min) by WES.

To conduct valid penetration studies, a special soil container was developed similar in material and shape to the standard Proctor Mold. This container consists of a hollow steel cylinder and base plate with dimensions as shown in figure 3. Photographs of the mold and its relative size may be found in figures C-3 and C-4 of appendix C.

The penetrometer data recording unit is comprised of a load cell, load cell power input source, and depth cell, all of which are connected to a data recording unit (and timer) on three separate channels. The load cell consists of a transducer located in the penetrometer cone head. The depth cell is composed of a 10-turn potentiometer and pulley system fastened to the boom of a moveable hoist and is operated by a wire cable attached to the penetrometer handle (fig. C-2). Automatic recording of data in the form of digital printed output (paper tape) was provided (fig. C-5). A schematic and diagram of the entire system is shown in figure 2.

Obstacle Specimens

Specifications for solid obstacles used in establishing penetration profiles are as follows.

1. Material: aluminum 6061-T6 alloy (machined)

2. Size and shape:

   a. Lower range: 2.54 by 2.54 centimeters (1 by 1 inch) circular right (ϕ) cylinder

   b. Middle range: 5.08 by 5.08 centimeters (2 by 2 inches) ϕ right cylinder

   c. Upper range: 7.62 by 7.62 centimeters (3 by 3 inches) ϕ right cylinder

The surface of each cylinder is concave on the loading face (that is, the face toward the penetrometer head) to ensure proper contact with the cone within the penetration influence area. Shape and relative size are illustrated in figure 4.

Specimens were placed at 15.24-, 30.48-, and 45.72-centimeter (6, 12, and 18 inch) depths within the mold. Depths were measured with respect to top of the mold and centerline of the obstacle (center of concavity). The profile centerline was located by means of a mold cover template. Relative size, depth, and location with respect to centerline of mold are shown in figure 4.

SUMMARY OF RESULTS

The relationships of obstacle displacement parameters are shown in figure 5. Original and final data are displayed in expanded form in table IV. Penetration resistance profiles of soils containing solid obstacles embedded within the soil matrix are shown in figures 6 to 23.

DISCUSSION OF RESULTS

Parametric Relationships

The values selected for the relationships between constant and variable parameters that were established previously are summarized in table V.

General Effects of Parameters

Effect of obstacles. - The penetration curves illustrated in figures 22 to 24 indicate that, at a specified depth, penetration resistance increases with increase in the size of the obstacle. This fact is reflected in table IV by the wide range of soil pressures exhibited with different size obstacles at the same depth. This is to be expected because the bearing capacity in cohesionless soils is known to increase with the diameter of the footing. Consequently, the force required to move the obstacle should be roughly proportional to the cube of the diameter.

With respect to displacement, smaller obstacles tend to be more easily displaced than larger ones, as evidenced by the values in table IV. One interesting observation is that for obstacles displaced laterally, the resistance profile does not return to the original curve, even in those cases in which the obstacle is completely removed from the path of the penetrometer. This phenomenon is explained by the fact that as pressure is applied through the obstacle by means of the penetrometer, the soil column directly below is densified. When the obstacle is finally displaced, this greater density effectively increases soil resistance, thus deviating the penetration profile. However, one would expect to return to the original profile eventually.

In the same curves mentioned previously, for a particular size of obstacle, greater depths generally result in greater deviations from the standard profile. Thus, the rate of force increase associated with encountering an obstacle tends to increase with increasing depth. The pressure differences between smallest and largest obstacle also increase with increasing depth, as shown in table IV.

Effect of grain size. - Comparison of the obstacle penetration curves for Standard Ottawa Sand and League City Sand at 50 percent relative density reveals that, in all cases with the same size and depth of obstacle, the greater resistance occurs in Ottawa Sand. One characteristic of the League City curves is the "spikes" produced. These spikes represent instantaneous high points of force and pressure and occur when the penetrometer either displaces the obstacle from its path or fails the soil directly beneath it, thus accelerating the obstacle downward. This is substantiated by the values of displacement listed in table IV. Another noticeable effect occurred when the obstacle was displaced by the penetrometer. In such cases, the tendency for the resistance curve to return to the original penetration profile was more pronounced for the finer grained League City Sand.

Effect of gradation. - The curves for League City Sand and AP-12 at 50 percent relative density indicate that for the same obstacle size and depth, gradation of the soil has little or no effect on penetration resistance. The only noticeable difference occurs with the 7.62- by 7.62-centimeter (3 by 3 inch) ϕ obstacle at the 15.24-centimeter

(6 inch) and 30.48-centimeter (12 inch) levels. Formation of high force peaks, more commonly referred to as "spiking," exists at these depths with AP-12 but not with League City Sand. The displacements in table IV support the fact that a well-graded soil becomes weaker with respect to depth than a uniform soil.

Effect of relative density. - The curves for Ottawa Sand of 25-, 50-, and 75-percent relative density (figs. 9 to 17) show that, for a constant size and depth of obstacle, penetration resistance increases with increase in relative density, as was expected. Values of displacements in table IV support this evidence. Some interesting observations noted from these curves are as follows.

1. In the case of spiking, greater peaks occurred with the larger values of relative density for a constant size and depth of obstacle.

2. For a given obstacle size and depth, as the relative density of the soil increases, the resistance force becomes greater at a faster rate.

Miscellaneous effects. - One significant observation was the phenomenon of "sensing" the obstacle before it was actually encountered. This is demonstrated by the sudden rise in resistance (force) at elevations well above those at which the obstacles were placed (for example, fig. 2). The stress field that precedes the penetrometer cone is altered by the presence of the rigid obstacle and this produces a greater penetration resistance, even before the obstacle is contacted.

Effects of Parameters in Terms of Work

The parameters analyzed in this study may be related by the concept of work. Generally, the work required by a vertical penetrometer to overcome the resistance of a buried solid obstacle is a function of the following variables.

D_o = diameter of obstacle

Z_o = depth of obstacle

D_s = average grain size (diameter) of the soil

G_s = grain-size distribution (gradation) of the soil

D_r = relative density of the soil

This work is equivalent to the area under the F-Z curve generated by an obstacle resistance profile for a particular set of variables. Stated mathematically,

$$W_R = f\left(D_o, Z_o, D_s, G_s, D_r\right) \tag{2}$$

$$W_R = f(Z)dZ = FdZ \quad (3)$$

where W_R = work necessary to overcome obstacle resistance and $F = f(Z)$ = vertically applied force.

Values of these integrals have been computed by planimeter measurement and were used to develop the quantitative relationships shown in figures 24 to 30. Significance of the results are discussed more thoroughly in the following sections.

Effect of obstacle size. - The curves in figure 24 illustrate that as the size of obstacle increases, the rate of change of work required increases in the direction of greater depth. In other words, the difference in work becomes greater between two lines of constant elevation (depth) as the size of the obstacle is increased, but this difference becomes greater at a more pronounced rate as the depth is increased. Another notable observation is that when the differences between any two pairs of elevations are equal (that is, 15.24- and 30.48-centimeter (6 and 12 inch) depths compared with 30.48- and 45.72-centimeter (12 and 18 inch) depths), the ratio of the differences in work required for constant obstacle size is approximately the same. The ratio for this particular set of curves is approximately 1.60.

Effect of obstacle depth. - The effects of varying depth are reciprocal to those of varying obstacle size; that is, as the depth of the obstacle increases, the rate of change of work required increases in the direction of increasing obstacle diameter, and when the differences between any two pairs of obstacle diameters are equal (2.54 centimeters (1 inch) ϕ and 5.08 centimeters (2 inches) ϕ compared with 5.08 centimeters (2 inches) ϕ and 7.62 centimeters (3 inches) ϕ), the ratio of the differences in work required is approximately a constant.

Effect of average grain size. - In figure 26, several important relationships are revealed concerning average grain size.

1. At the same depth, the work required to overcome an obstacle of constant size increases with increasing average grain size.

2. At equal depths, the rate of change of work required with respect to increasing obstacle size is constant and not dependent on average grain size.

3. For a constant obstacle size, the difference in work required between any two elevations (depths) increases with increasing average grain size.

Effect of gradation. - Because the uniformity coefficient of AP-12 is approximately three times that of League City Sand, the two soils may be considered to represent a fairly wide latitude of gradations. However, the curves in figure 27 show that at equal depth (for a constant obstacle size), only slightly more work is required in League City Sand than in AP-12. It also appears as though the rate of change of work required with respect to increasing obstacle size is approximately the same for both soils along lines of equal elevation. Thus, there is no pronounced effect on penetration resistance for the range of gradations tested (uniformity coefficient = 1.90 to 6.17).

Effects of relative density. - The curves illustrated in figures 28 to 30 bear significant results with respect to relative density. For constant depth, the following statements are true.

1. The work required increases with increasing relative density for a constant obstacle size.

2. The rate of change of work required with respect to increasing obstacle size increase with increasing relative density.

3. For equal differerences in relative density (that is, D_r = 25 and 50 percent, 50 and 75 percent, and so forth), the ratio of the differences in work required is essentially constant for the same size obstacle and is approximately equal to 1.00.

For varying depth, the following statements are true.

1. For a constant relative density, the rate of change of work required with respect to increasing obstacle size increases at a greater rate as the depth increases.

2. The ratio of the differences in work required between two relative densities at any depth and for a constant obstacle size is approximately a constant.

CONCLUSIONS AND RECOMMENDATIONS

With respect to penetration resistance in cohesionless soils, the conclusions established from this study are as follows. At a given depth and with respect to a soil of known gradation and relative density, penetration resistance increases with increase in obstacle size, or more specifically, with increase in mean diameter. For a given size of obstacle and with respect to a soil of known gradation and relative density, penetration resistance increases with the increase in depth of the obstacle. For a given size and depth of obstacle and with respect to a soil of known gradation and relative density, penetration resistance increases with increase in (average) grain size. For a given size and depth of obstacle and with respect to a soil of known relative density, gradation has little effect on penetration resistance for the range of gradations tested (uniformity coefficient = 1.90 to 6.17). For a given size and depth of obstacle and with respect to a soil of known gradation, penetration resistance increases with increase in relative density.

With respect to buried obstacles, parameters possibly affecting penetration resistance in a soil that have not been included in this study are the following.

1. Penetrometer size and shape (cone compared to plate)

2. Rate of penetration

3. Interference levels or perpendicular distance between the penetrometer axis and the center of mass of an obstacle

The effects of these parameters should be thoroughly analyzed and relationships established similar to those found in this study. It is expected that such an analysis will effectively complete the Soil Penetration Resistance Study program.

The concept of work required to overcome obstacles established earlier in this paper should be expanded to include effects of the new parameters just discussed. Then, this work relationship essentially will become a common denominator for the entire set of parameters analyzed.

Manned Spacecraft Center
National Aeronautics and Space Administration
Houston, Texas, November 9, 1972
914-50-15-06-72

REFERENCES

1. Terzaghi, Karl; and Peck, Ralph B.: Soil Mechanics in Engineering Practice. Second ed., John Wiley and Sons, 1967.

2. Anon.: Soils Penetration Resistance Study Program (SPERS). Lockheed Electronics Company Document 645D.21.068, Feb. 1971.

3. Mitchell, J. K.; Bromwell, L. G.; Carrier, W. D., III; Costes, N. C.; and Scott, R. F.: Soil Mechanics Experiment. Section 4, Apollo 14 Preliminary Science Report, NASA SP-272, June, 1971.

4. Terzaghi, Karl: Theoretical Soil Mechanics. First ed., John Wiley and Sons, 1952.

5. Lambe, T. William: Soil Testing for Engineers. First ed., John Wiley and Sons, 1965.

6. Anon.: Effect of Mold Size and Other Factors on Laboratory Cone Index Measurements. Waterways Experiment Station, United States Army Corps of Engineers, M.P. No. 4-327, Mar. 1959.

TABLE I. - DENSITY-RELATIVE DENSITY RELATIONSHIPS

Soil type	γ_{max}, N/m^3 (lb/ft^3)	γ_{min}, N/m^3 (lb/ft^3)	γ - D_r equation (a)
Medium Sand	18 947 (120.6)	15 491 (98.6)	$D_r = \frac{18\,947}{\gamma} \times \frac{\gamma - 15\,491}{3456} \times 100$ percent
Ottawa Sand	17 266 (109.9)	15 177 (96.6)	$D_r = \frac{17\,266}{\gamma} \times \frac{\gamma - 15\,177}{2089} \times 100$ percent
League City Sand	15 648 (99.6)	12 585 (80.1)	$D_r = \frac{15\,648}{\gamma} \times \frac{\gamma - 12\,585}{3063} \times 100$ percent
Lunar simulant	18 665 (118.8)	14 266 (90.8)	$D_r = \frac{18\,665}{\gamma} \times \frac{\gamma - 14\,266}{4399} \times 100$ percent

[a]Equation shown for only one system of units.

TABLE II. - RANGES OF D_r USED IN CURVE DEVELOPMENT

Soil	Relative density D_r, percent				
MS	0	25	50	--	100
OS	0	25	50	75	100
LCS	--	25	50	75	100
AP-12	--	35	50	65	85

TABLE III. - TERRESTRIAL MOISTURE CONTENTS

Soil	Moisture content, percent
MS	0.025
OS	.035
LCS	.060
AP-12	.010

TABLE IV. - DATA MATRIX

Soil type	Obstacle size, cm (in.)														
	2.54 by 2.54 (1 by 1)[a]					5.08 by 5.08 (2 by 2)[b]					7.62 by 7.62 (3 by 3)[c]				
	Displacement parameter[d]					Displacement parameter[d]					Displacement parameter[d]				
	V, cm (in.)	H, cm (in.)	α, deg	F_m, N (lb)	p_m, N/cm^2 (lb/in.^{2})	V, cm (in.)	H, cm (in.)	α, deg	F_m, N (lb)	p_m, N/cm^2 (lb/in.^{2})	V, cm (in.)	H, cm (in.)	α, deg	F_m, N (lb)	p_m, N/cm^2 (lb/in.^{2})
Bendix MS[e]															
Relative density D_r = 25 percent															
Density γ = 16 245 N/m^3 (103.4 lb/ft^3)															
Depth of obstacle, cm (in.)															
15.24 (6)	5.08 (2)	2.54 (1)	10	350.2 (78.7)	68.1 (100.2)	(f)	(f)	(f)	487.3 (109.5)	23.7 (34.9)	(f)	(f)	(f)	536.2 (120.5)	11.6 (17.0)
30.48 (12)	5.08 (2)	2.54 (1)	90	486.4 (109.3)	94.7 (139.2)	(f)	(f)	(f)	299.9 (67.4)	14.6 (21.5)	(f)	(f)	(f)	451.2 (101.4)	9.7 (14.3)
45.72 (18)	5.08 (2)	(f)	(f)	481.9 (108.3)	93.8 (137.9)	(f)	(f)	(f)	340.4 (76.5)	16.6 (24.4)	(f)	(f)	(f)	371.1 (83.4)	8.0 (11.8)
Standard Ottawa Sand[e]															
Relative density D_r = 25 percent															
Density γ = 15 648 N/m^3 (99.6 lb/ft^3)															
Depth of obstacle, cm (in.)															
15.24 (6)	5.08 (2)	2.54 (1)	90	142.4 (32.0)	27.7 (40.7)	8.89 (3.5)	(f)	(f)	222.1 (49.9)	10.8 (15.9)	2.54 (1)	(f)	(f)	400.1 (89.9)	8.6 (12.7)
30.48 (12)	2.54 (1)	2.54 (1)	80	131.3 (29.5)	25.6 (37.6)	3.81 (1.5)	1.27 (0.5)	10	242.1 (54.4)	11.8 (17.3)	2.54 (1)	(f)	(f)	348.9 (78.4)	7.5 (11.1)
45.72 (18)	5.08 (2)	2.54 (1)	90	142.0 (31.9)	27.6 (40.6)	2.54 (1)	2.54 (1)	(f)	252.3 (56.7)	12.2 (18.0)	2.54 (1)	(f)	(f)	326.6 (73.4)	7.1 (10.4)
Relative density D_r = 50 percent															
Density γ = 16 151 N/m^3 (102.8 lb/ft^3)															
Depth of obstacle, cm (in.)															
15.24 (6)	3.81 (1.5)	2.54 (1)	90	683.5 (120.6)	104.4 (153.6)	3.81 (1.50)	(f)	60	383.6 (86.2)	18.6 (27.4)	(f)	(f)	(f)	450.8 (101.3)	9.7 (14.3)
30.48 (12)	3.81 (1.5)	1.27 (0.5)	90	354.7 (62.6)	54.2 (79.7)	(f)	(f)	(f)	398.7 (89.6)	19.4 (28.5)	(f)	(f)	(f)	510.9 (114.8)	11.0 (16.2)
45.72 (18)	2.54 (1)	1.27 (.5)	90	396.5 (70.0)	60.6 (89.1)	(f)	(f)	(f)	462.8 (104.0)	22.5 (33.1)	(f)	(f)	(f)	574.5 (129.1)	12.4 (18.3)
Relative density D_r = 75 percent															
Density γ = 16 685 N/m^3 (106.2 lb/ft^3)															
Depth of obstacle, cm (in.)															
15.24 (6)	2.54 (1)	2.54 (1)	45	589.5 (104.0)	90.0 (132.4)	3.81 (1.5)	(f)	(f)	419.2 (94.2)	20.4 (30.0)	2.54 (1)	(f)	(f)	251.9 (56.6)	5.4 (8.0)
30.48 (12)	(f)	1.27 (.5)	75	603.4 (106.5)	92.2 (135.6)	(f)	(f)	(f)	485.5 (109.1)	23.6 (34.7)	(f)	(f)	(f)	483.7 (108.7)	10.5 (15.4)
45.72 (18)	(f)	1.27 (.5)	90	396.1 (69.9)	60.5 (89.0)	(f)	(f)	(f)	536.2 (120.5)	26.1 (38.4)	(f)	(f)	(f)	579.8 (130.3)	12.5 (18.4)
League City Sand[e]															
Relative density D_r = 50 percent															
Density γ = 13 951 N/m^3 (88.8 lb/ft^3)															
Depth of obstacle cm (in.)															
15.24 (6)	10.16 (4)	2.54 (1)	90	230.5 (40.7)	35.2 (51.8)	10.16 (4)	2.54 (1)	90	127.7 (28.7)	6.2 (9.1)	3.81 (1.5)	(f)	(f)	210.0 (47.2)	4.6 (6.7)
30.48 (12)	10.16 (4)	2.54 (1)	85	166.4 (29.4)	25.4 (37.4)	6.35 (2.5)	(f)	(f)	84.1 (18.9)	4.1 (6.0)	5.08 (2)	(f)	(f)	460.1 (103.4)	9.9 (14.6)
45.72 (18)	5.08 (2)	2.54 (1)	90	96.1 (17.0)	14.7 (21.6)	2.54 (1)	1.27 (0.5)	80	159.8 (35.9)	7.8 (11.4)	2.54 (1)	20.32 (8.0)	0.5	528.7 (118.8)	11.4 (16.8)
AP-12[g]															
Relative density D_r = 50 percent															
Density γ = 16 072 N/m^3 (102.3 lb/ft^3)															
Depth of obstacle, cm (in.)															
15.24 (6)	15.24 (6)	2.54 (1)	90	56.1 (9.9)	8.6 (12.6)	11.43 (4.5)	2.54 (1)	90	116.1 (26.1)	5.6 (8.3)	10.16 (4)	1.27 (0.5)	45	88.1 (19.8)	1.9 (2.8)
30.48 (12)	10.16 (4)	2.54 (1)	90	113.4 (20.0)	17.3 (25.5)	10.16 (4)	2.54 (1)	90	137.5 (30.9)	6.7 (9.8)	8.89 (3.5)	1.27 (.5)	60	89.0 (20.0)	1.9 (2.8)
45.72 (18)	10.16 (4)	(f)	(f)	294.3 (51.9)	44.9 (66.1)	7.62 (3)	(f)	(f)	407.2 (91.5)	19.8 (29.1)	5.08 (2)	(f)	(f)	36.5 (81.0)	7.8 (11.5)

[a]Obstacle area = 5.06740 cm^2 (0.78540 in.^{2}), obstacle volume = 12.87270 cm^3 (0.78540 in.^{3}), and obstacle weight = 0.34236 N (0.07697 lb).

[b]Obstacle area = 7.06859 cm^2 (3.14160 in.^{2}), obstacle volume = 102.98164 cm^3 (6.28320 in.^{3}), and obstacle weight = 2.73885 N (0.61575 lb).

[c]Obstacle area = 45.60654 cm^2 (7.06859 in.^{2}), obstacle volume = 347.56257 cm^3 (21.20577 in.^{3}), and obstacle weight = 6.19237 N (1.39217 lb).

[d]Obstacle area = $\pi D_o^2/4$ and obstacle volume = $\pi D_o^2 H_o/4$, where D_o = obstacle diameter and H_o = obstacle height; obstacle weight = $\gamma_o(V_o)$, where γ_o = obstacle density and V_o = obstacle volume; and maximum pressure, $p_m = F_m/A_o$, where F_m = maximum vertical force and A_o = obstacle area.

[e]Gradation = uniform.

[f]Negligible displacement.

[g]Gradation = well graded.

TABLE V. - RELATION OF EXPERIMENTAL PARAMETERS

<table>
<tr><td rowspan="2">Parameter constant</td><td colspan="17">Parameter varied</td></tr>
<tr><td colspan="3">Obstacle size, cm (in.)</td><td colspan="3">Obstacle depth, cm (in.)</td><td colspan="3">Relative density D_r, percent</td><td colspan="4">Grain size</td><td colspan="4">Gradation</td></tr>
<tr><td>Soil type</td><td colspan="3">OS</td><td colspan="3">OS</td><td colspan="3">OS</td><td colspan="2">MS</td><td colspan="2">LCS</td><td colspan="2">LCS</td><td colspan="2">AP-12</td></tr>
<tr><td rowspan="3">Obstacle size, cm (in.)</td><td>2.54 ϕ (1)</td><td>5.08 ϕ (2)</td><td>7.62 ϕ (3)</td><td rowspan="3">2.54 ϕ (1)</td><td rowspan="3">5.08 ϕ (2)</td><td rowspan="3">7.62 ϕ (3)</td><td rowspan="3">2.54 ϕ (1)</td><td rowspan="3">5.08 ϕ (2)</td><td rowspan="3">7.62 ϕ (3)</td><td rowspan="3">2.54 ϕ (1)</td><td rowspan="3" colspan="2">5.08 ϕ (2)</td><td rowspan="3">7.62 ϕ (3)</td><td rowspan="3">2.54 ϕ (1)</td><td rowspan="3" colspan="2">5.08 ϕ (2)</td><td rowspan="3">7.62 ϕ (3)</td></tr>
<tr><td>2.54 ϕ (1)</td><td>5.08 ϕ (2)</td><td>7.62 ϕ (3)</td></tr>
<tr><td>2.54 ϕ (1)</td><td>5.08 ϕ (2)</td><td>7.62 ϕ (3)</td></tr>
<tr><td rowspan="3">Obstacle depth, cm (in.)</td><td colspan="3">15.24 (6)</td><td>15.24 (6)</td><td>15.24 (6)</td><td>45.72 (18)</td><td colspan="3">15.24 (6)</td><td colspan="4">15.24 (6)</td><td colspan="4">15.24 (6)</td></tr>
<tr><td colspan="3">30.48 (12)</td><td>15.24 (6)</td><td>30.48 (12)</td><td>45.72 (18)</td><td colspan="3">30.48 (12)</td><td colspan="4">30.48 (12)</td><td colspan="4">30.48 (12)</td></tr>
<tr><td colspan="3">45.72 (18)</td><td>15.24 (6)</td><td>45.72 (18)</td><td>45.72 (18)</td><td colspan="3">45.72 (18)</td><td colspan="4">45.72 (18)</td><td colspan="4">45.72 (18)</td></tr>
<tr><td>Relative density D_r, percent</td><td colspan="3">50</td><td colspan="3">50</td><td>25</td><td>50</td><td>75</td><td colspan="4">50</td><td colspan="4">50</td></tr>
<tr><td>Grain size</td><td colspan="3">Medium</td><td colspan="3">Medium</td><td colspan="3">Medium</td><td colspan="2">Medium</td><td colspan="2">Small</td><td colspan="4">Small</td></tr>
<tr><td>Gradation</td><td colspan="3">Uniform</td><td colspan="3">Uniform</td><td colspan="3">Uniform</td><td colspan="4">Uniform</td><td colspan="2">Uniform</td><td colspan="2">Well graded</td></tr>
</table>

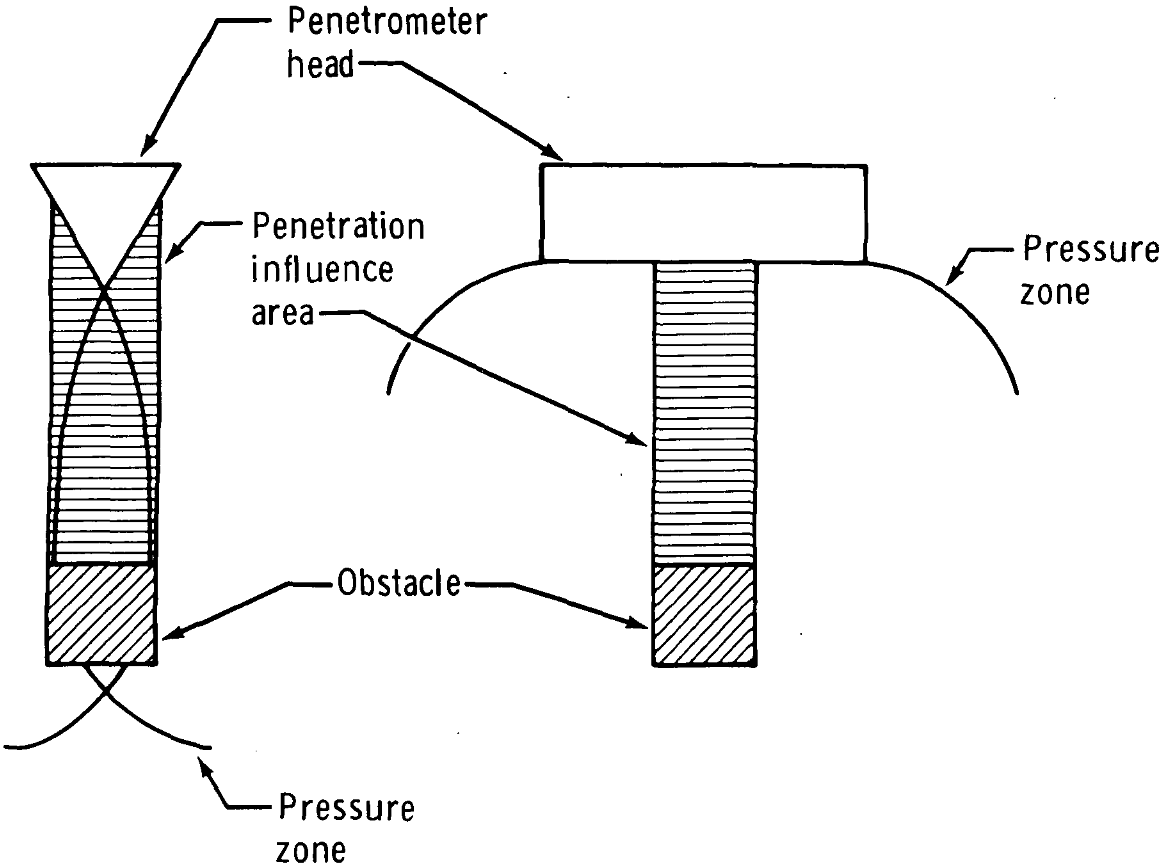

Figure 1.- Penetration influence area.

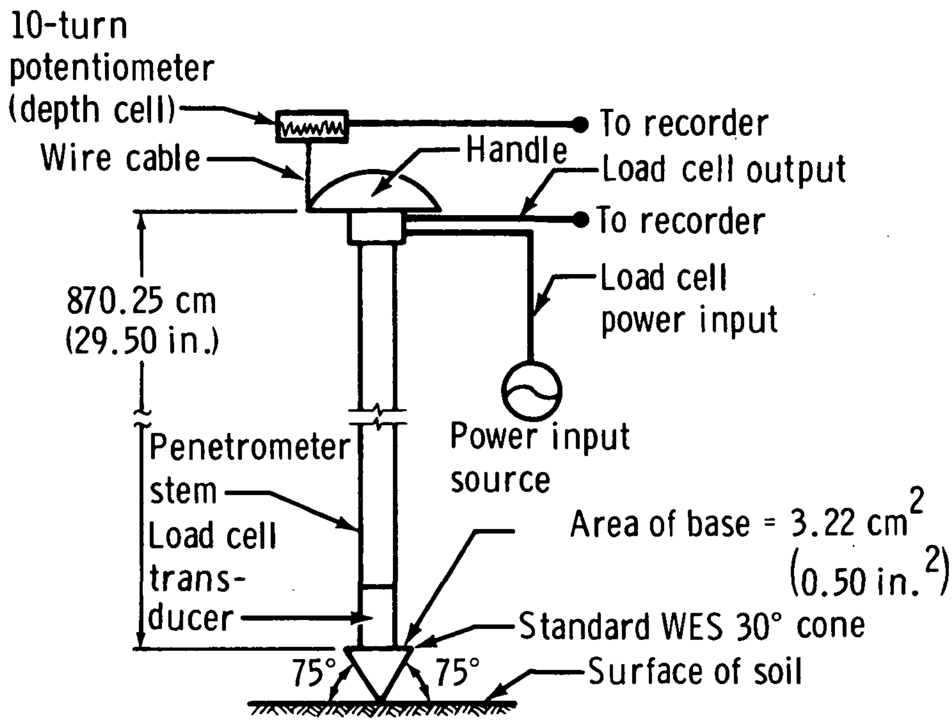

Figure 2. - Standard penetrometer.

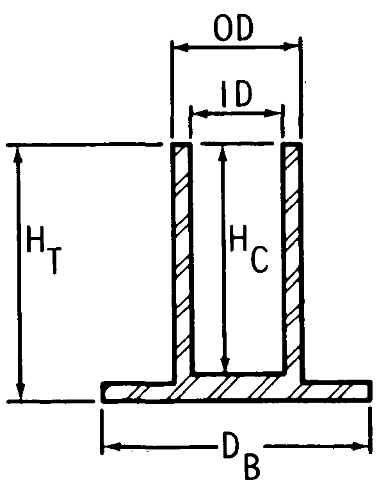

OD = outside diameter of cylinder = 39.62 cm (15.60 in.)
ID = inside diameter of cylinder = 37.08 cm (14.60 in.)
H_C = height of cylinder = 91.44 cm (36.00 in.)
H_T = total height of mold = 92.96 cm (36.60 in.)
D_B = diameter of base plate = 47.24 cm (18.60 in.)
V_M = volume of mold = 0.09 m^3 (3.48 ft^3)

Figure 3. - Standard mold.

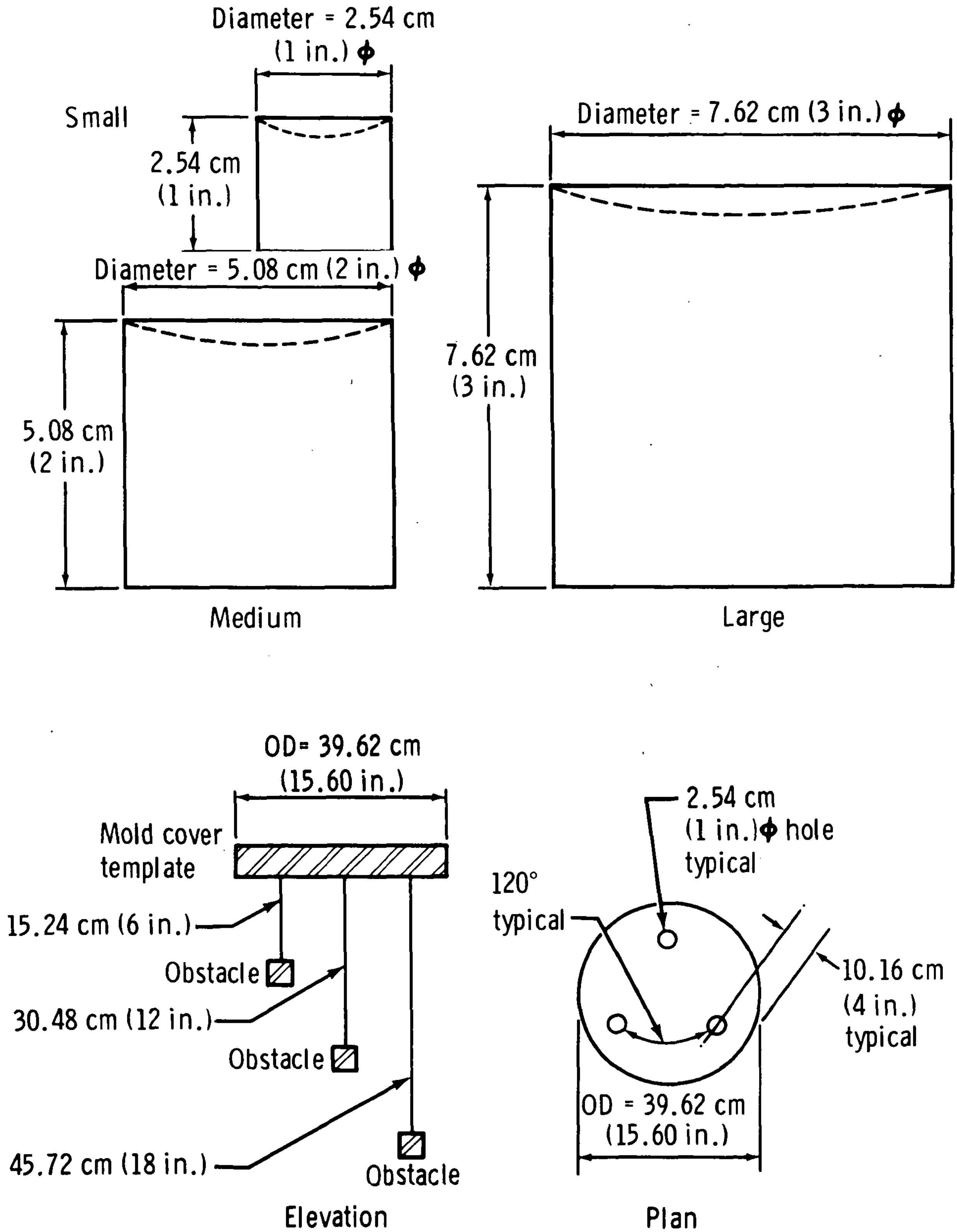

Figure 4. - Obstacle size range (actual size) and placement diagram.

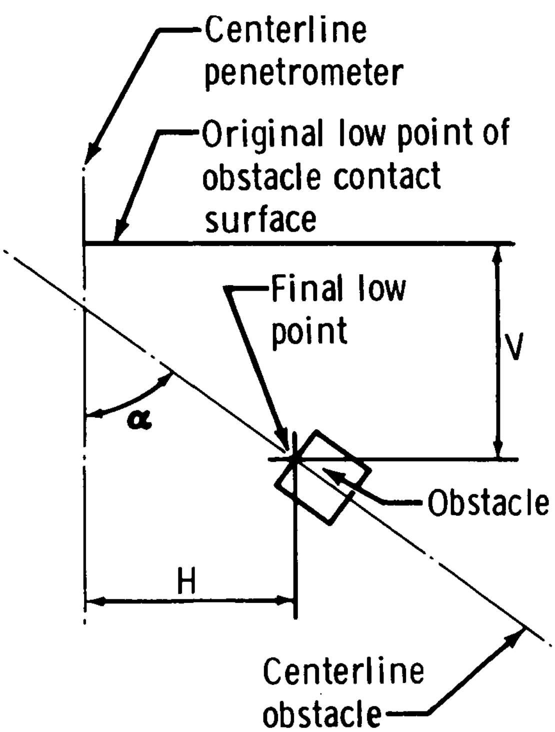

Description of displacement variables

1. Vertical displacement, V:
   Vertical distance measured from original to final centerline at low-point of obstacle contact surface
2. Horizontal displacement, H:
   Horizontal distance measured from centerline of penetration to final centerline at low point of obstacle contact surface
3. Displacement angle, a:
   Angle between centerline of obstacle
4. Maximum vertical force, F_m:
   Maximum verticle force exerted on penetrometer head
5. Maximum soil pressure, P_m:
   Maximum vertical pressure exerted by the soil on the base of the penetrometer cone

Figure 5. - Obstacle displacement parameters.

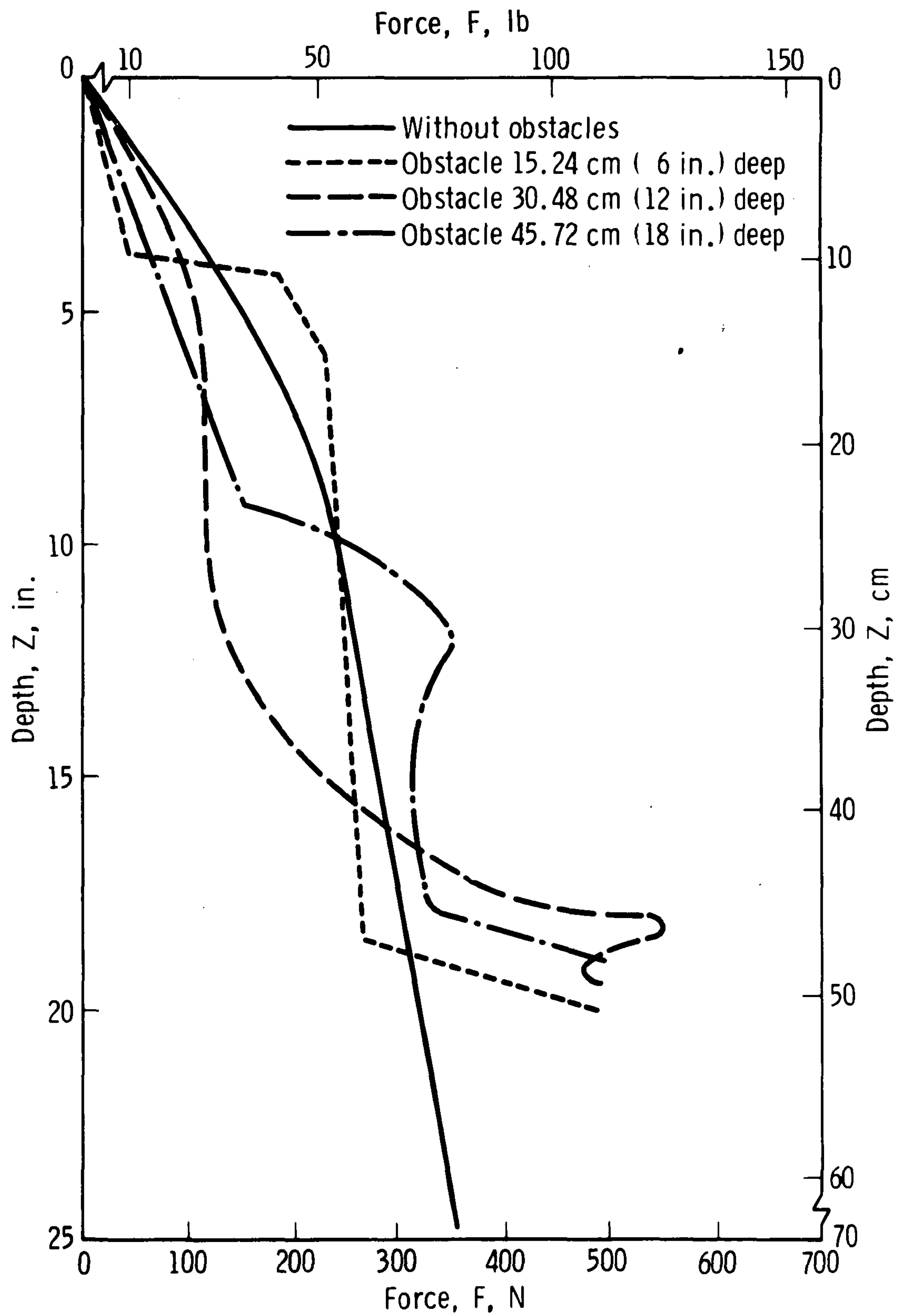

Figure 6. - Penetration resistance profiles with 2.54- by 2.54-cm (1 by 1 in.) obstacles in Bendix Medium Sand (D_r = 25 percent).

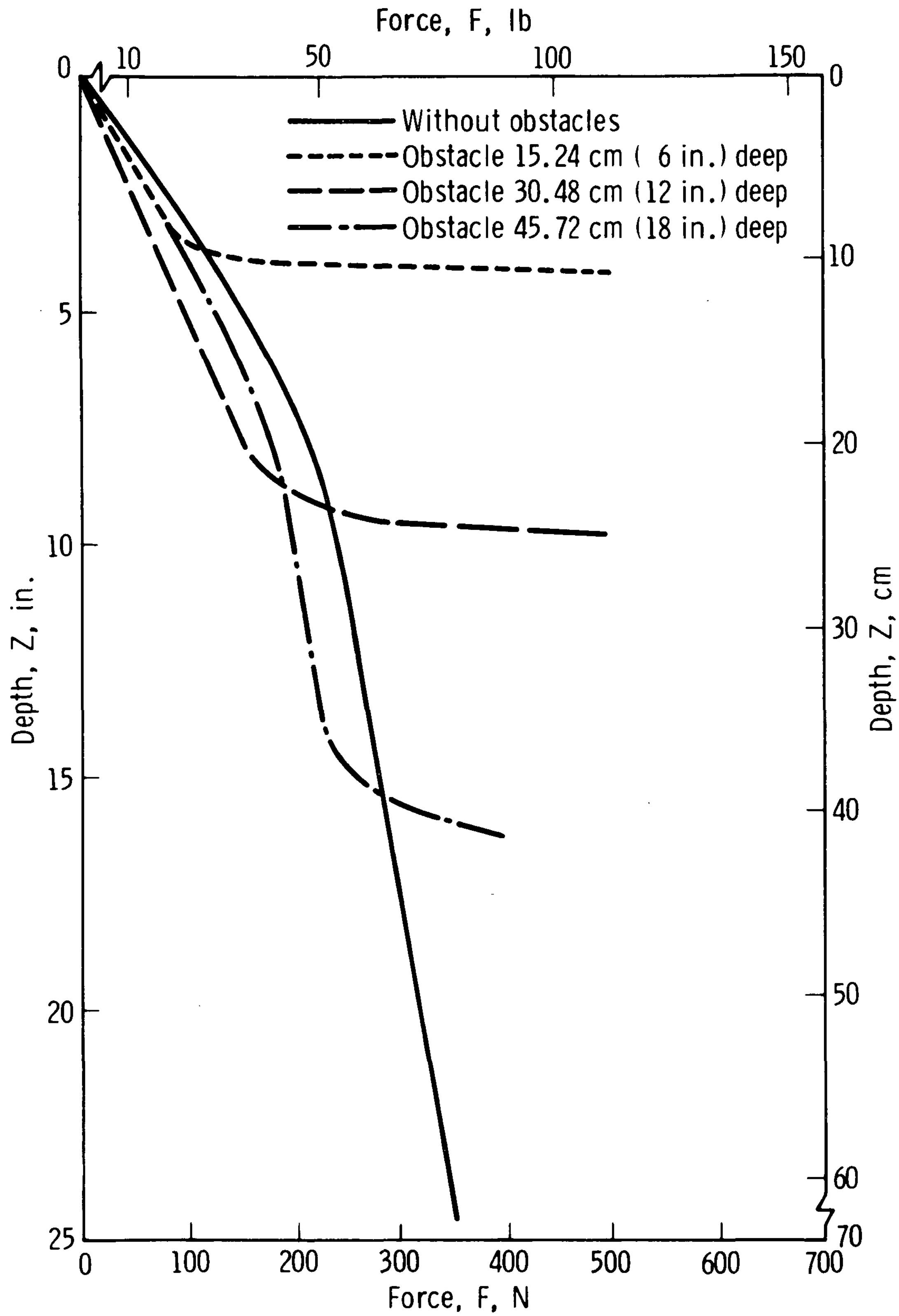

Figure 7. - Penetration resistance profiles with 5.08- by 5.08-cm (2 by 2 in.) obstacles in Bendix Medium Sand (D_r = 25 percent).

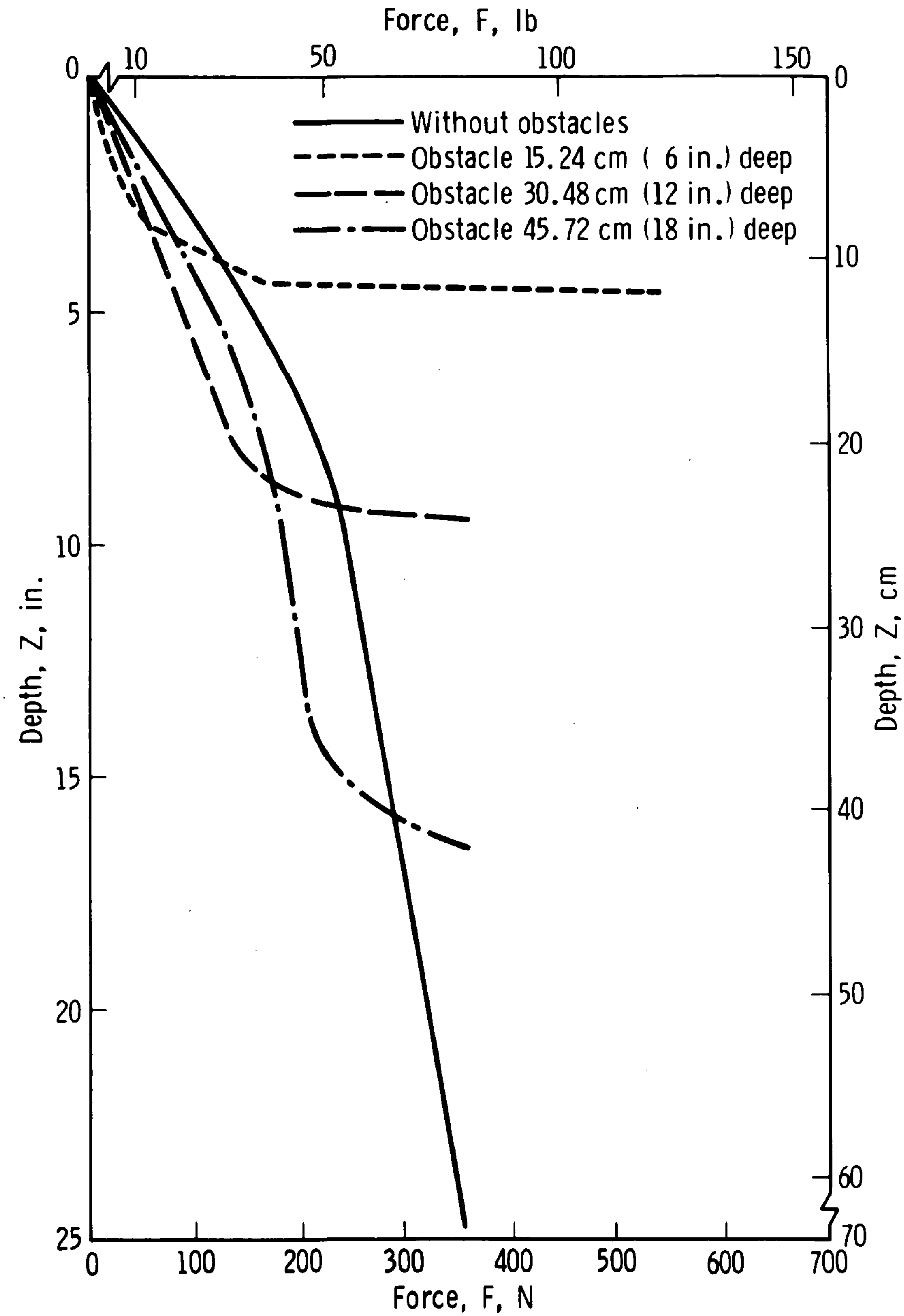

Figure 8. - Penetration resistance profiles with 7.62- by 7.62-cm (3 by 3 in.) obstacles in Bendix Medium Sand (D_r = 25 percent).

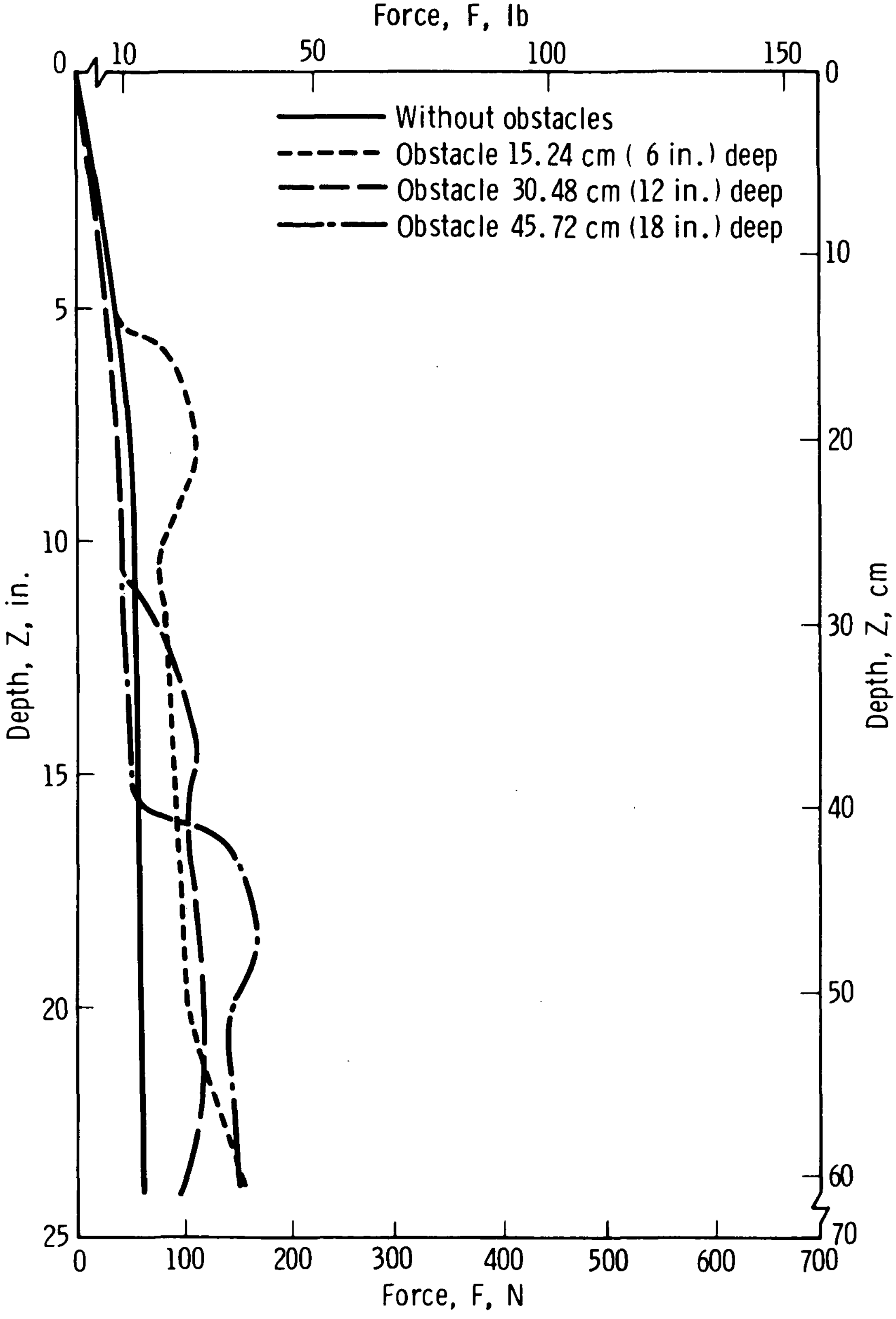

Figure 9.- Penetration resistance profiles with 2.54- by 2.54-cm (1 by 1 in.) obstacles in Standard Ottawa Sand (D_r = 25 percent).

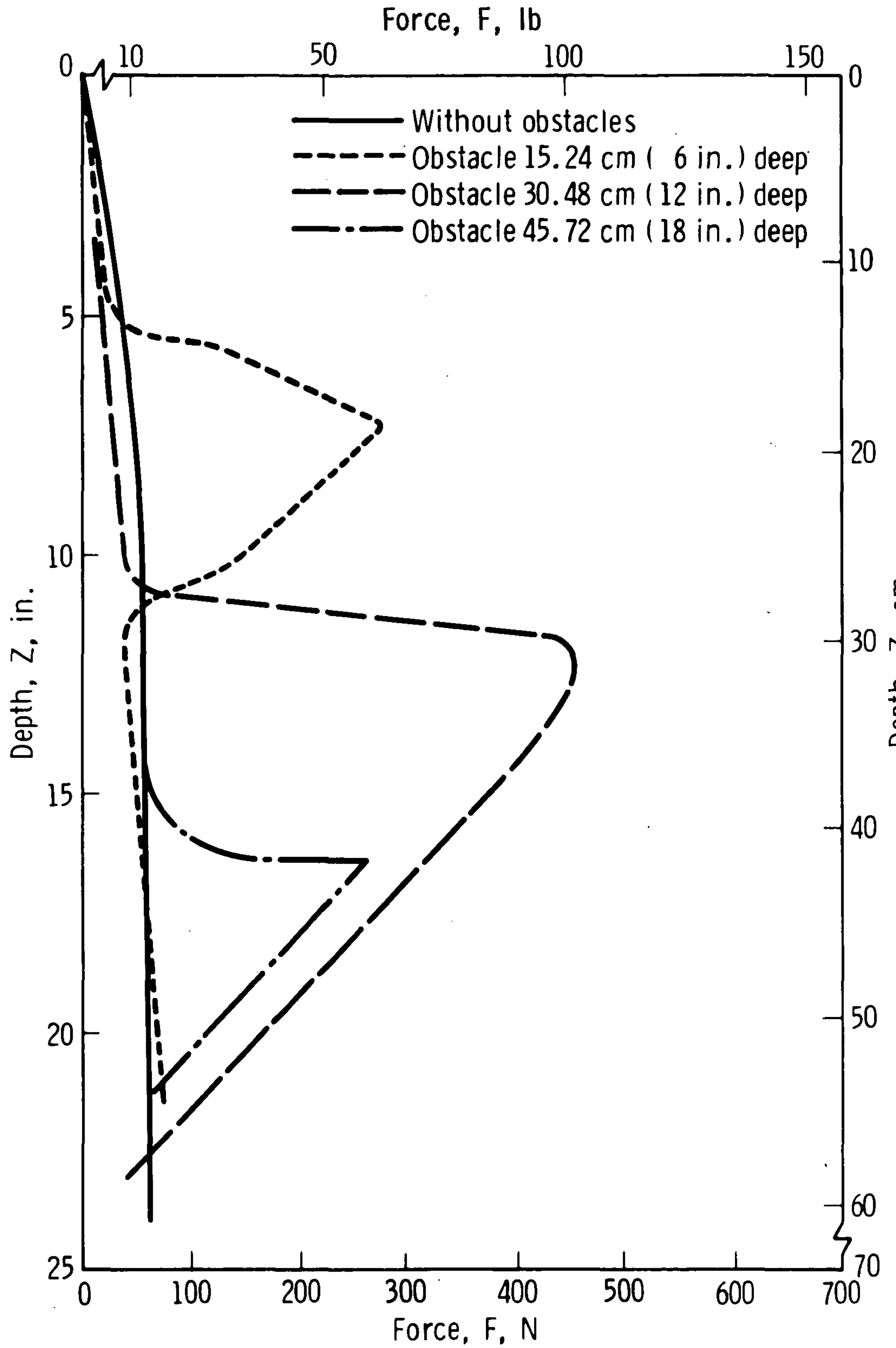

Figure 10. - Penetration resistance profiles with 5.08- by 5.08-cm (2 by 2 in.) obstacles in Standard Ottawa Sand (D_r = 25 percent).

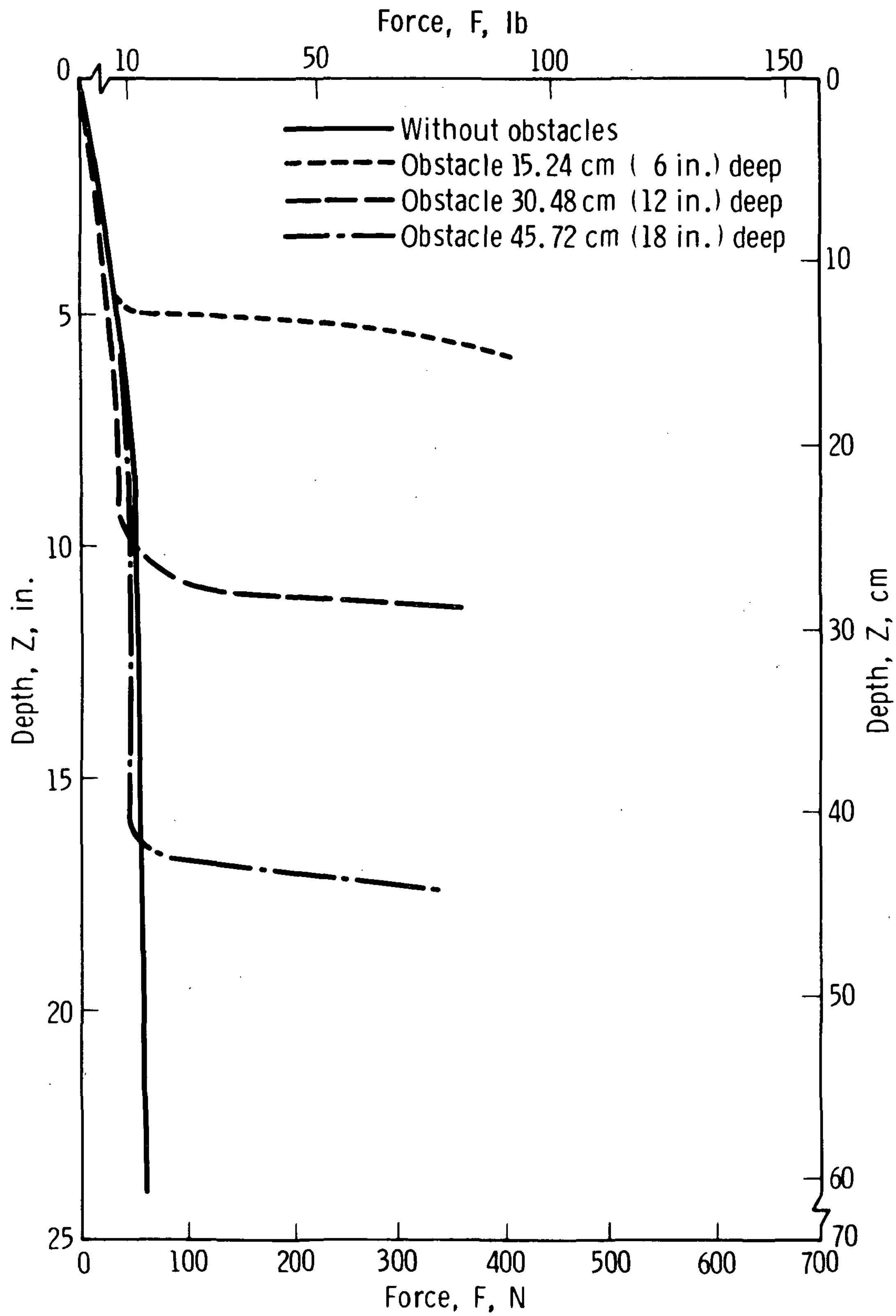

Figure 11. - Penetration resistance profiles with 7.62- by 7.62-cm (3 by 3 in.) obstacles in Standard Ottawa Sand (D_r = 25 percent).

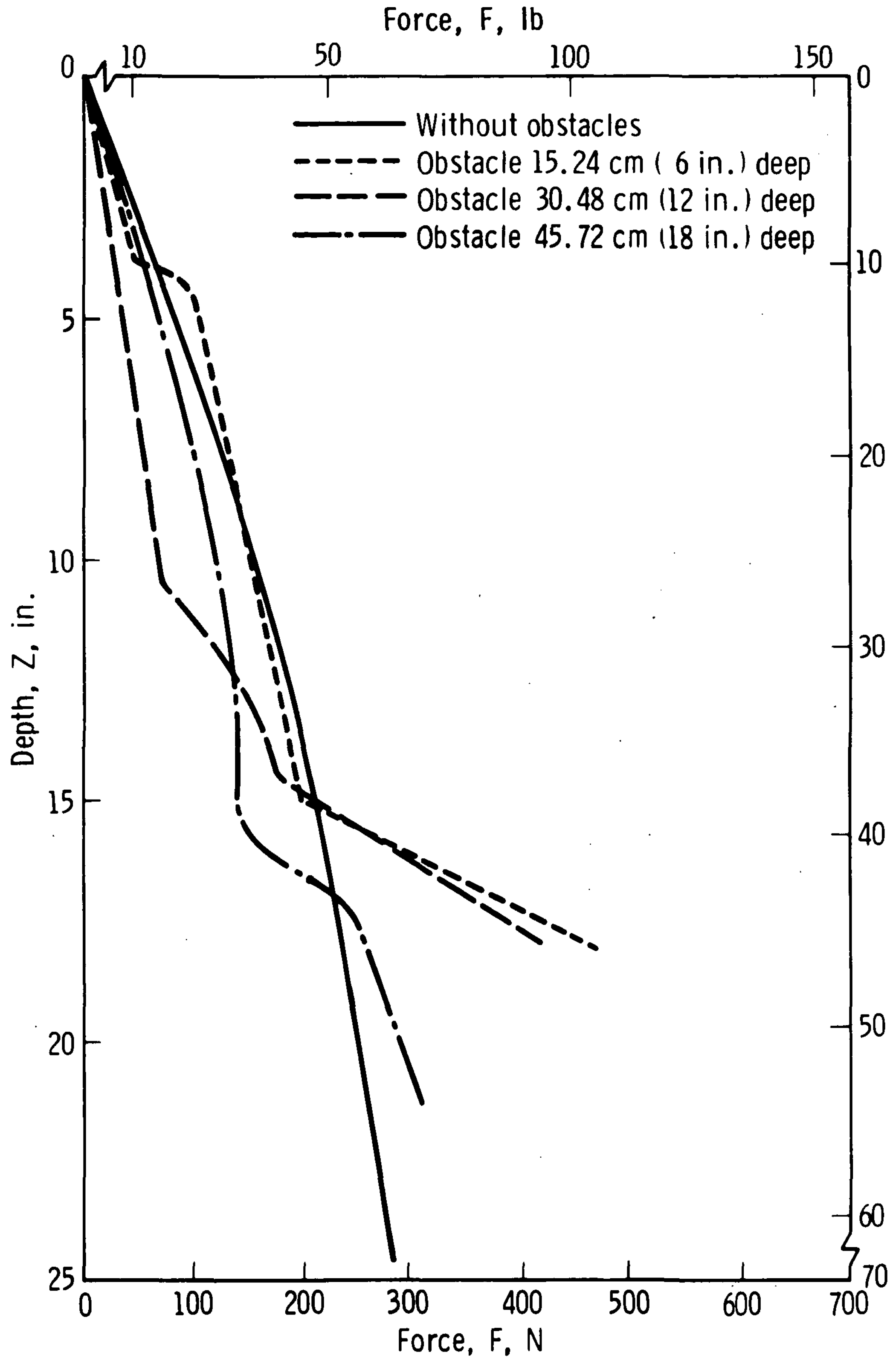

Figure 12. - Penetration resistance profiles with 2.54- by 2.54-cm (1 by 1 in.) obstacles in Standard Ottawa Sand (D_r = 50 percent).

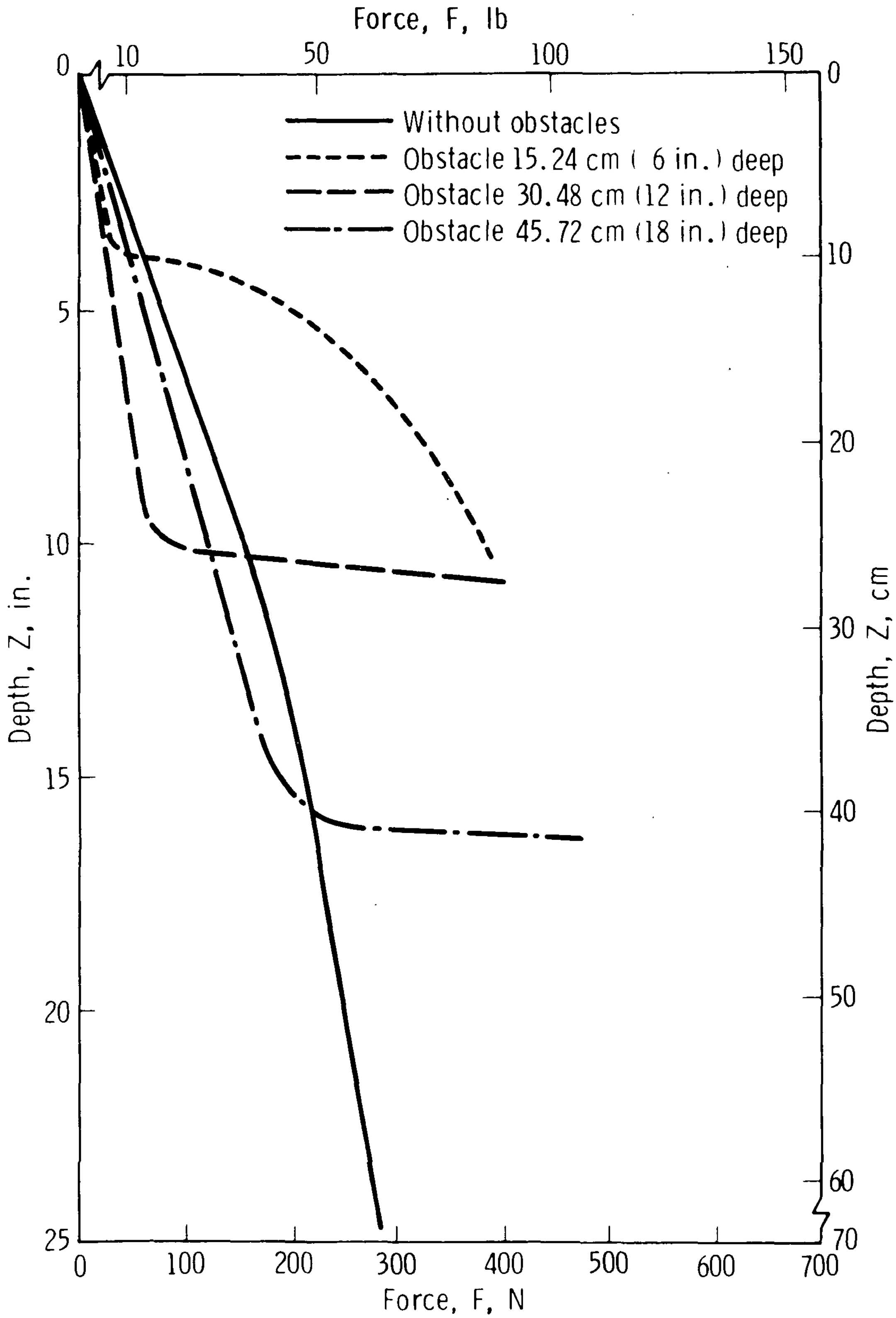

Figure 13.- Penetration resistance profiles with 5.08- by 5.08-cm (2 by 2 in.) obstacles in Standard Ottawa Sand (D_r = 50 percent).

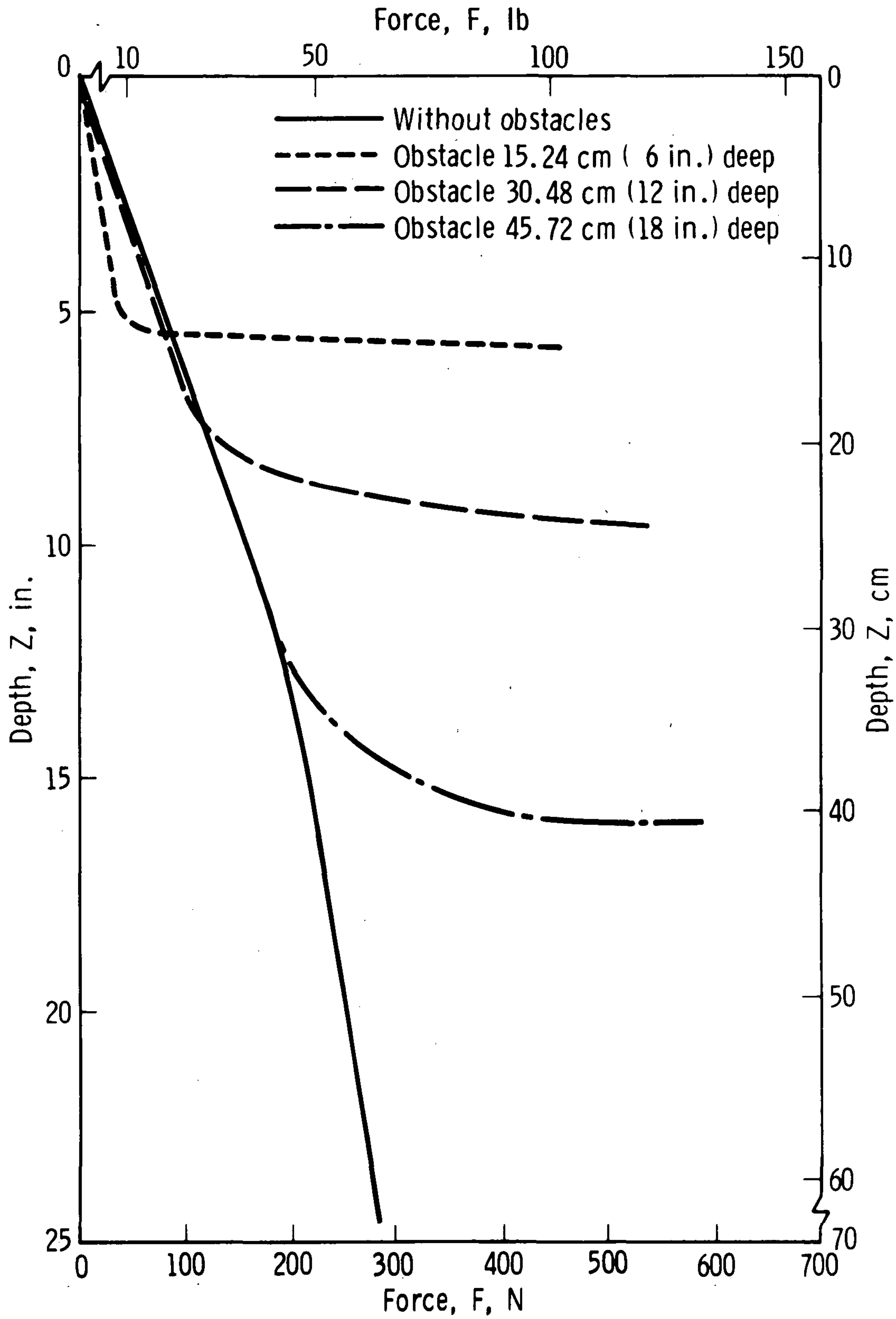

Figure 14. - Penetration resistance profiles with 7.62- by 7.62-cm (3 by 3 in.) obstacles in Standard Ottawa Sand (D_r = 50 percent).

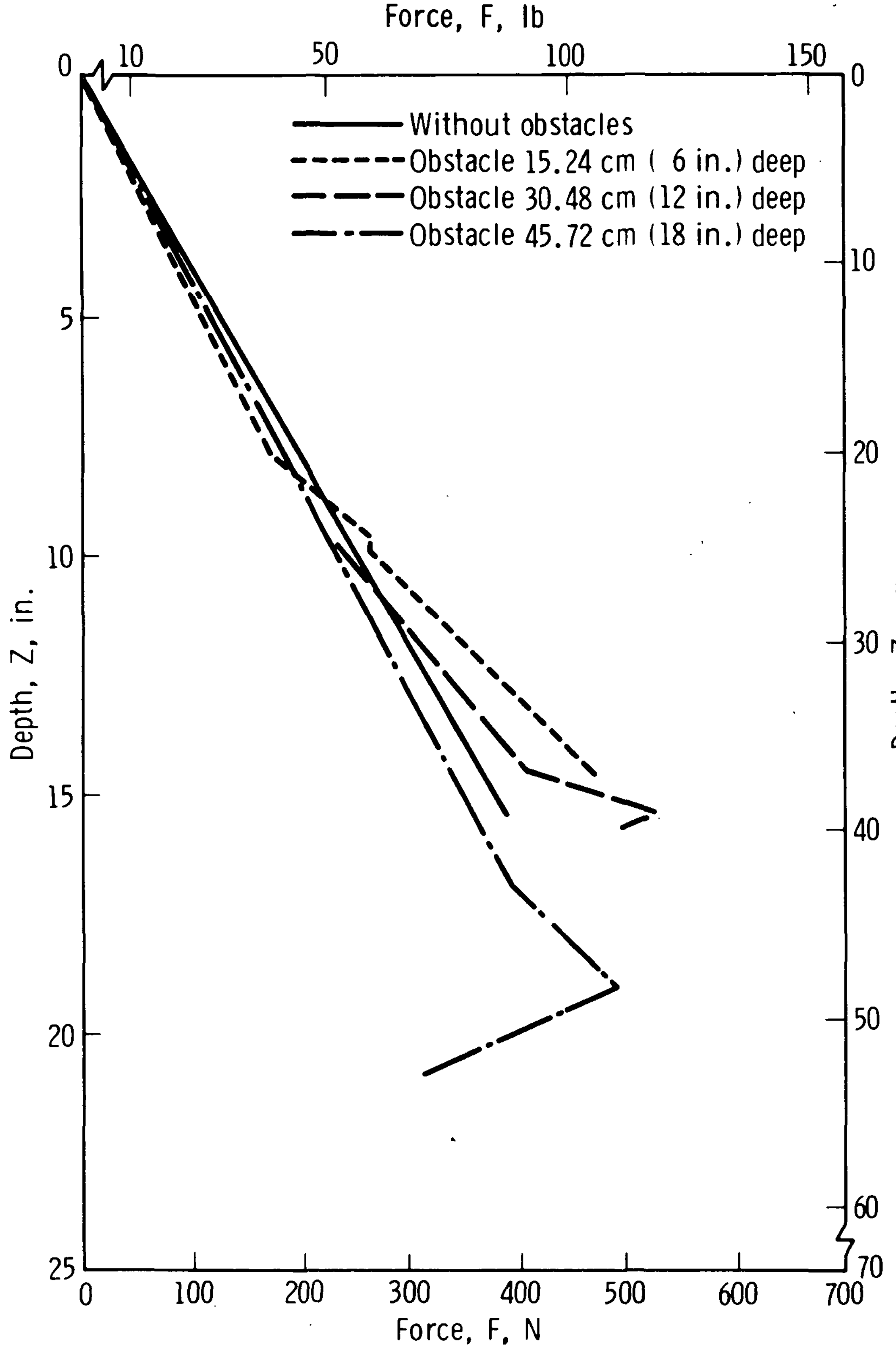

Figure 15.- Penetration resistance profiles with 2.54- by 2.54-cm (1 by 1 in.) obstacles in Standard Ottawa Sand (D_r = 75 percent).

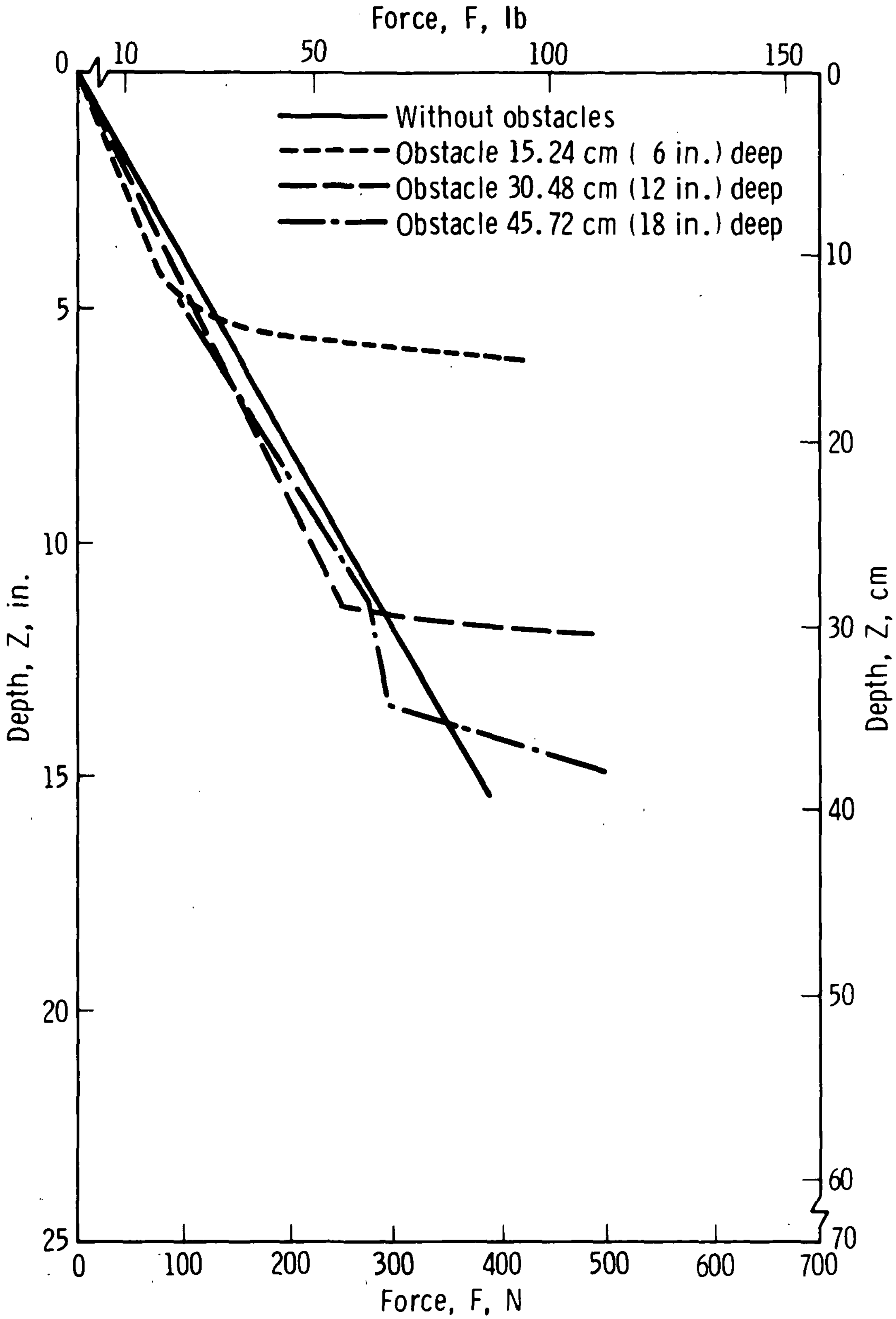

Figure 16.- Penetration resistance profiles with 5.08- by 5.08-cm (2 by 2 in.) obstacles in Standard Ottawa Sand (D_r = 75 percent).

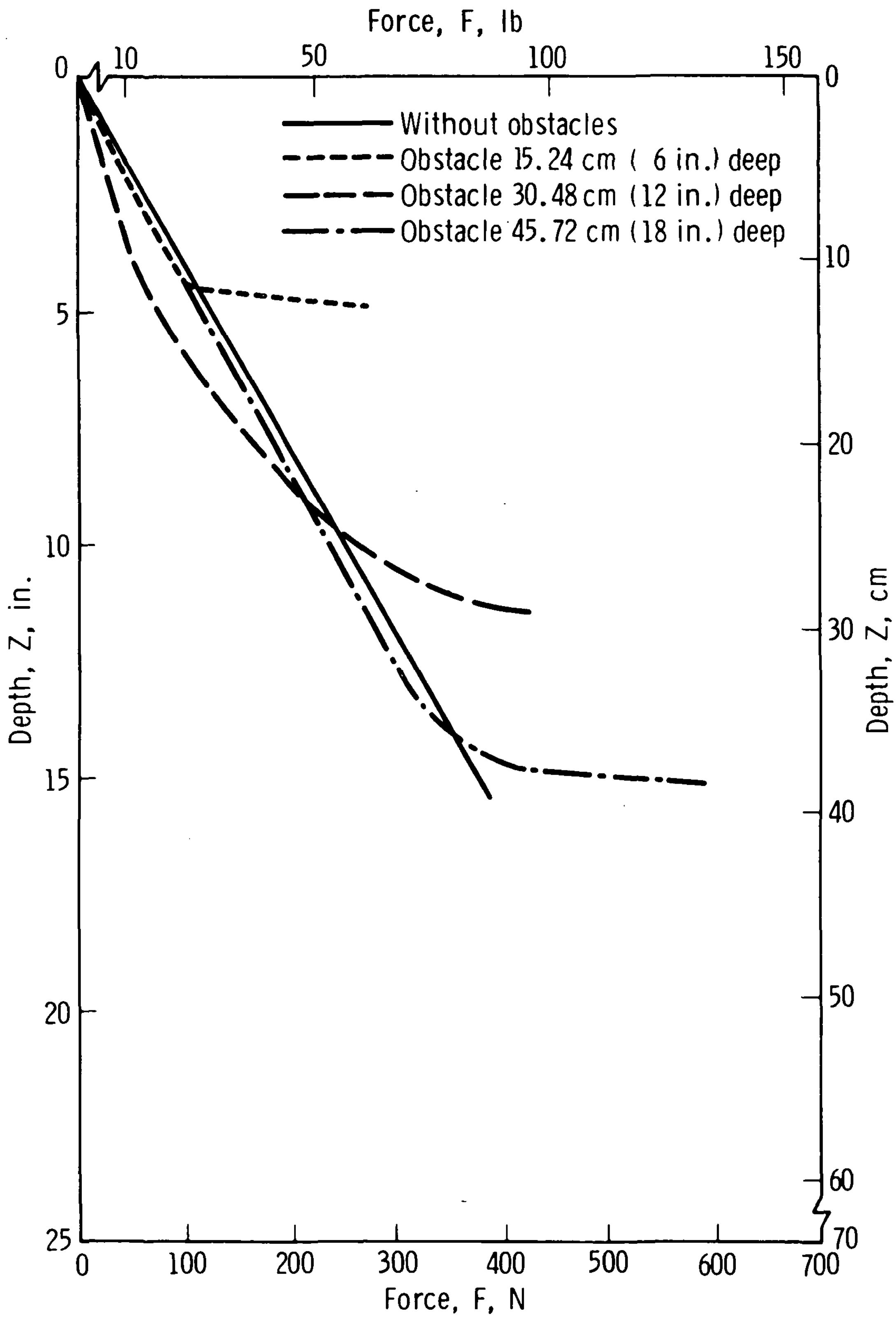

Figure 17. - Penetration resistance profiles with 7.62- by 7.62-cm (3 by 3 in.) obstacles in Standard Ottawa Sand (D_r = 75 percent).

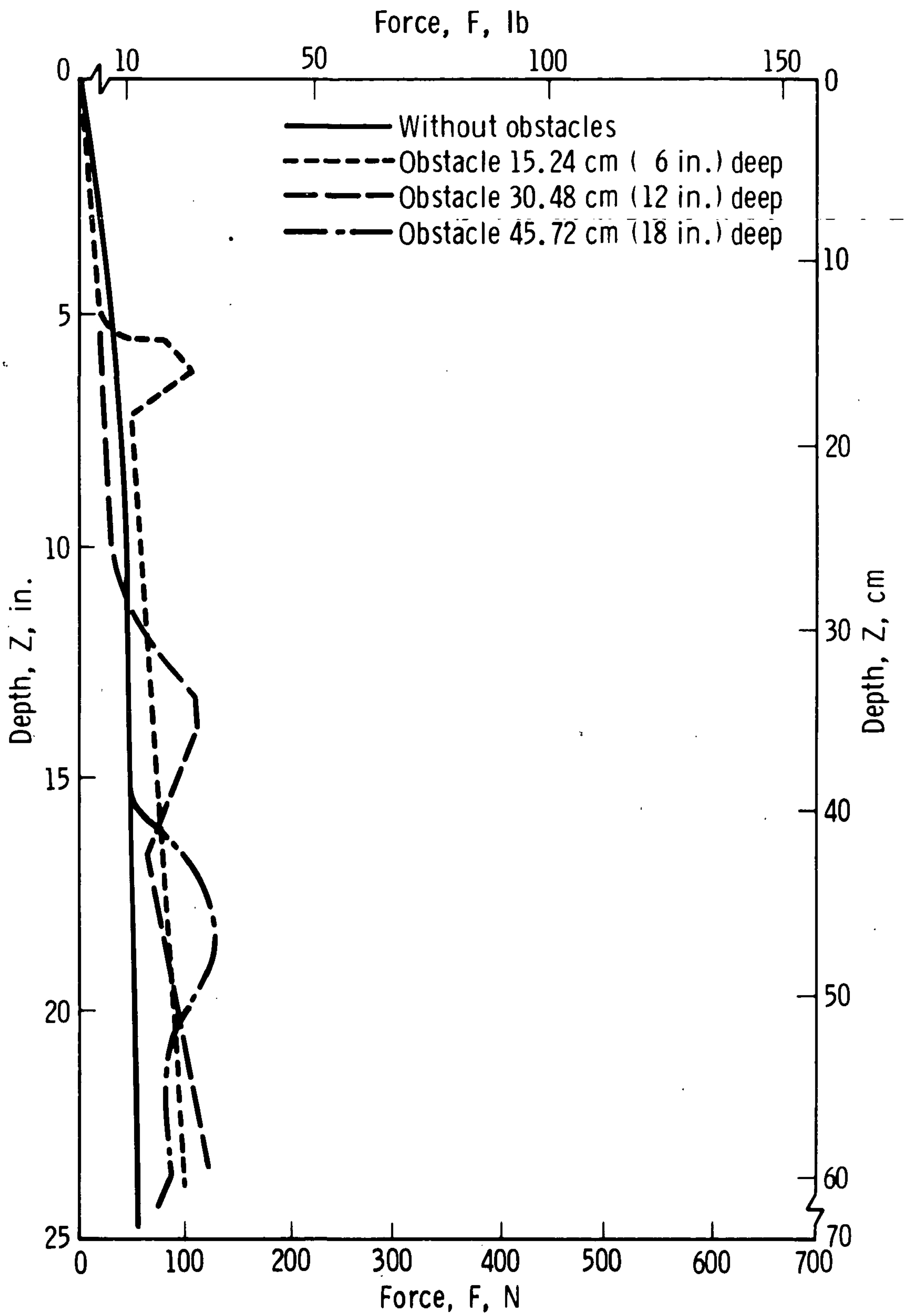

Figure 18.- Penetration resistance profiles with 2.54- by 2.54-cm (1 by 1 in.) obstacles in League City Sand (D_r = 50 percent).

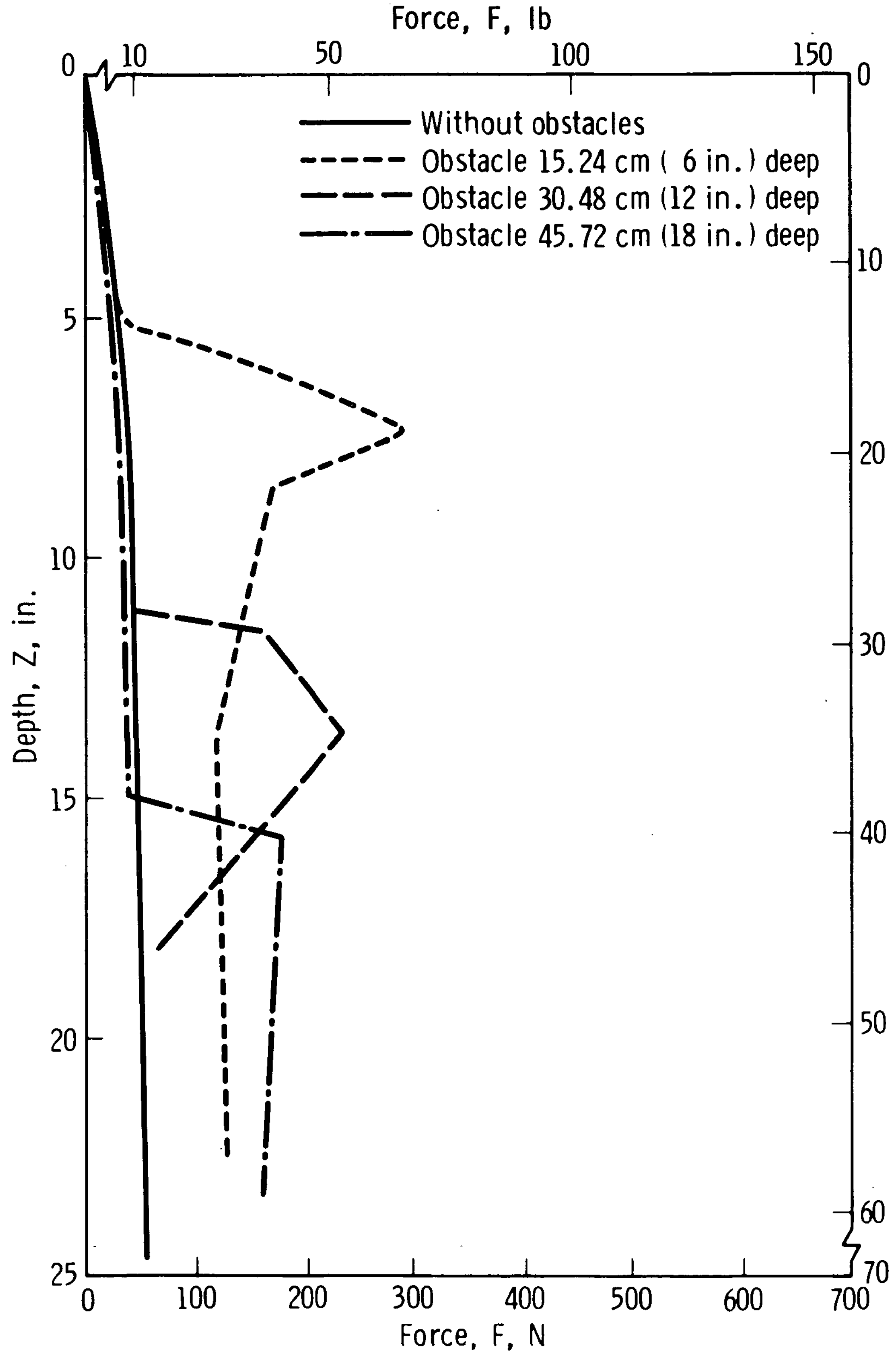

Figure 19.- Penetration resistance profiles with 5.08- by 5.08-cm (2 by 2 in.) obstacles in League City Sand (D_r = 50 percent).

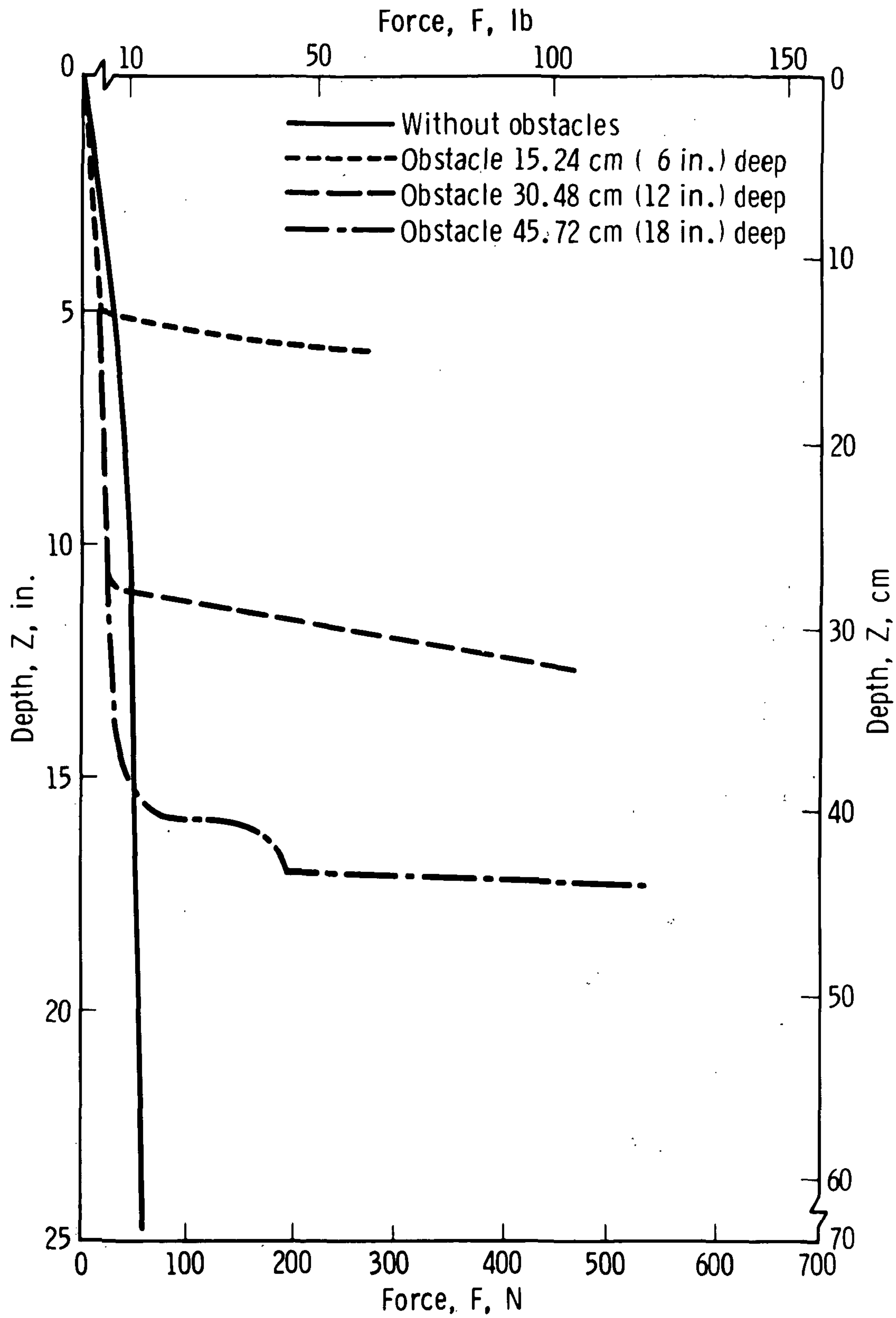

Figure 20. - Penetration resistance profiles with 7.62- by 7.62-cm (3 by 3 in.) obstacles in League City Sand (D_r = 50 percent).

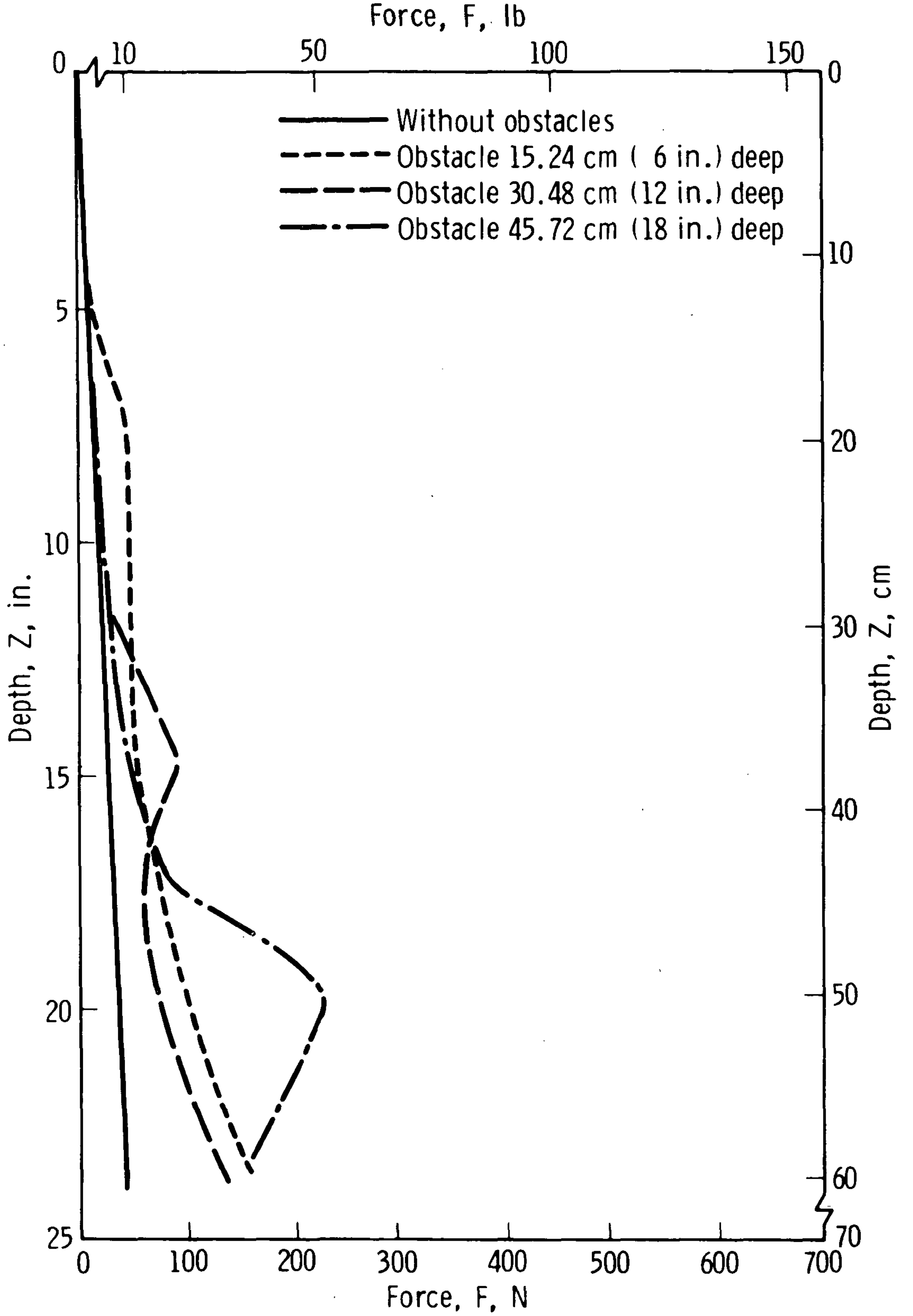

Figure 21. - Penetration resistance profiles with 2.54- by 2.54-cm (1 by 1 in.) obstacles in AP-12 (D_r = 50 percent).

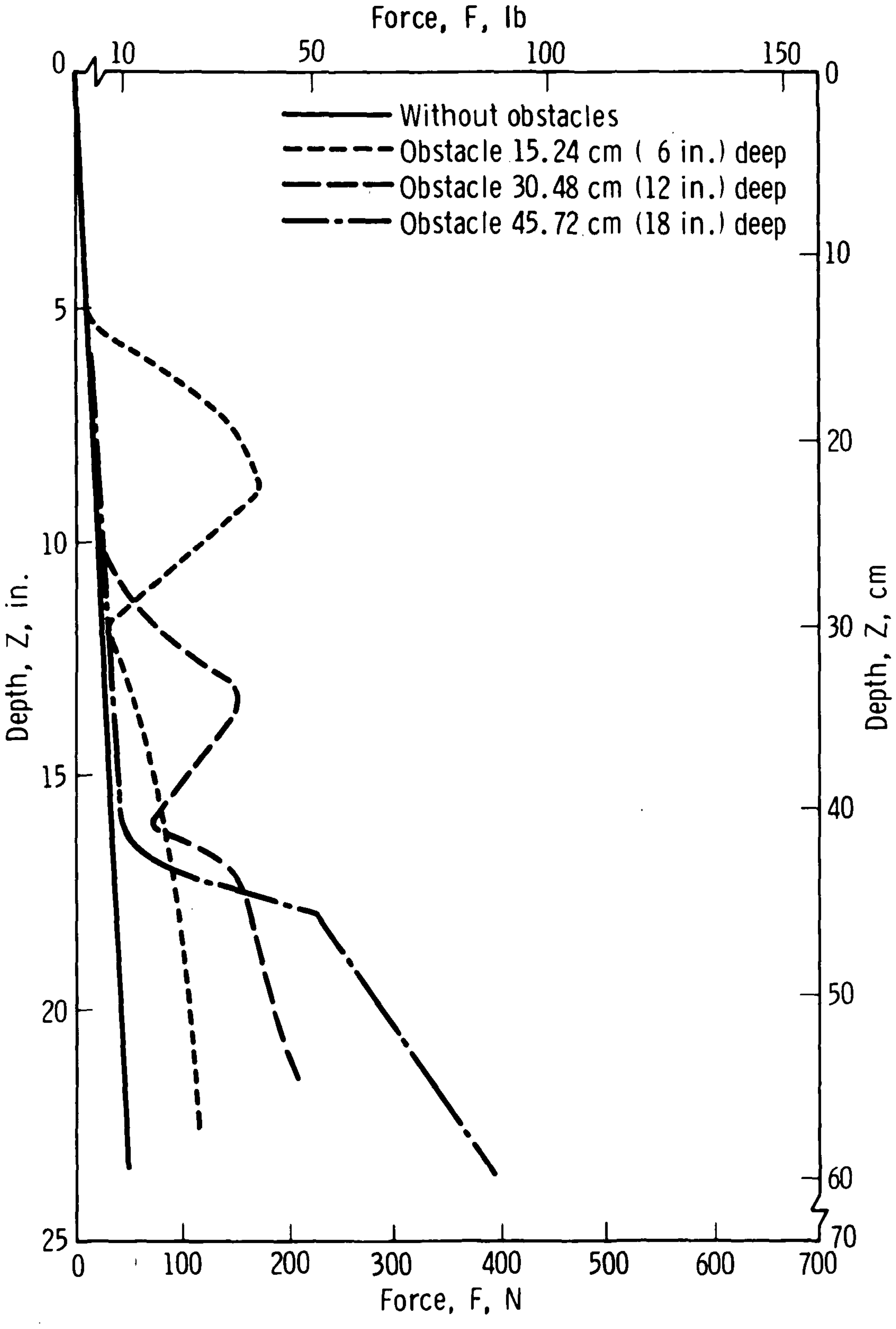

Figure 22. - Penetration resistance profiles with 5.08- by 5.08-cm (2 by 2 in.) obstacles in AP-12 (D_r = 50 percent).

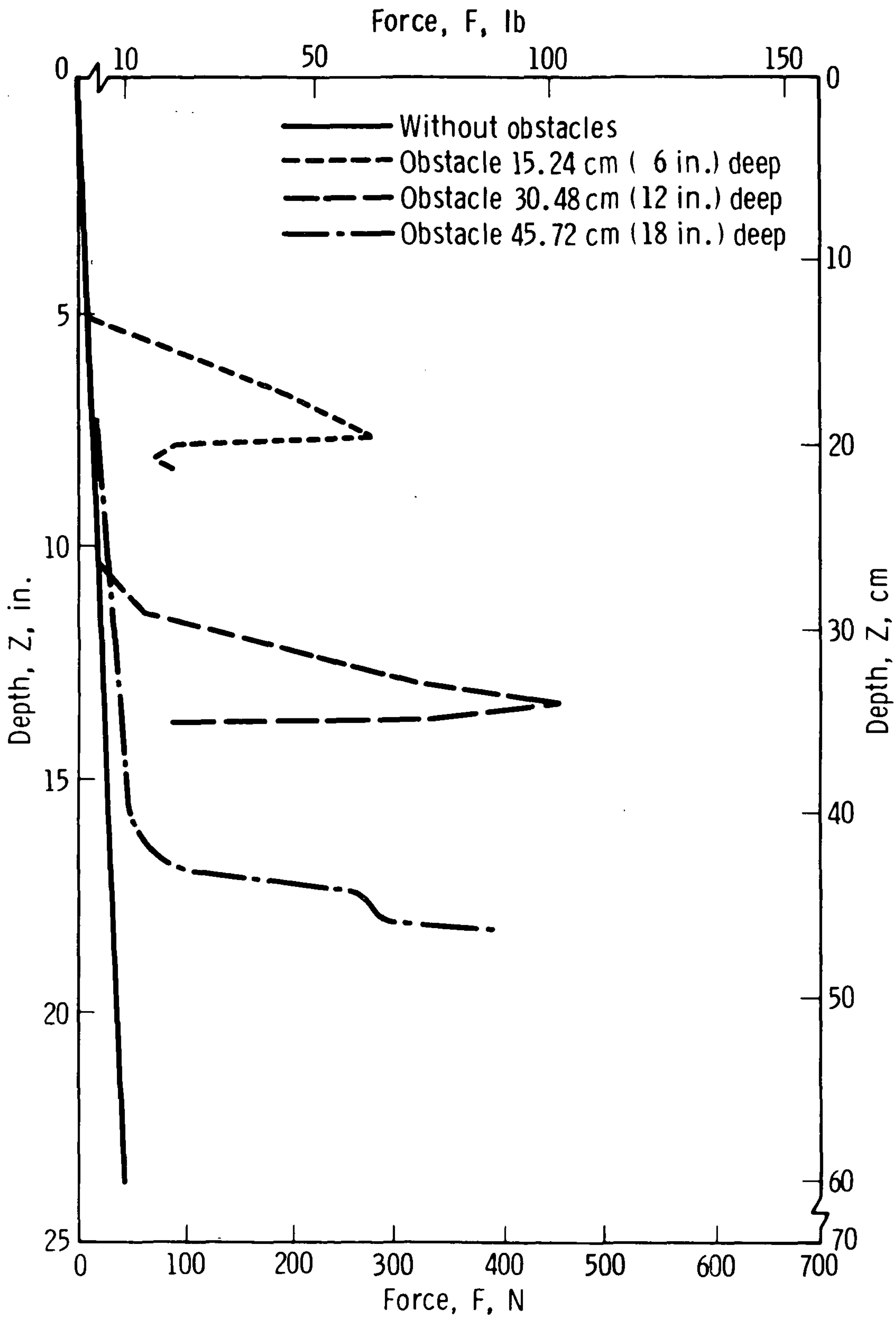

Figure 23. - Penetration resistance profiles with 7.62- by 7.62-cm (3 by 3 in.) obstacles in AP-12 (D_r = 50 percent).

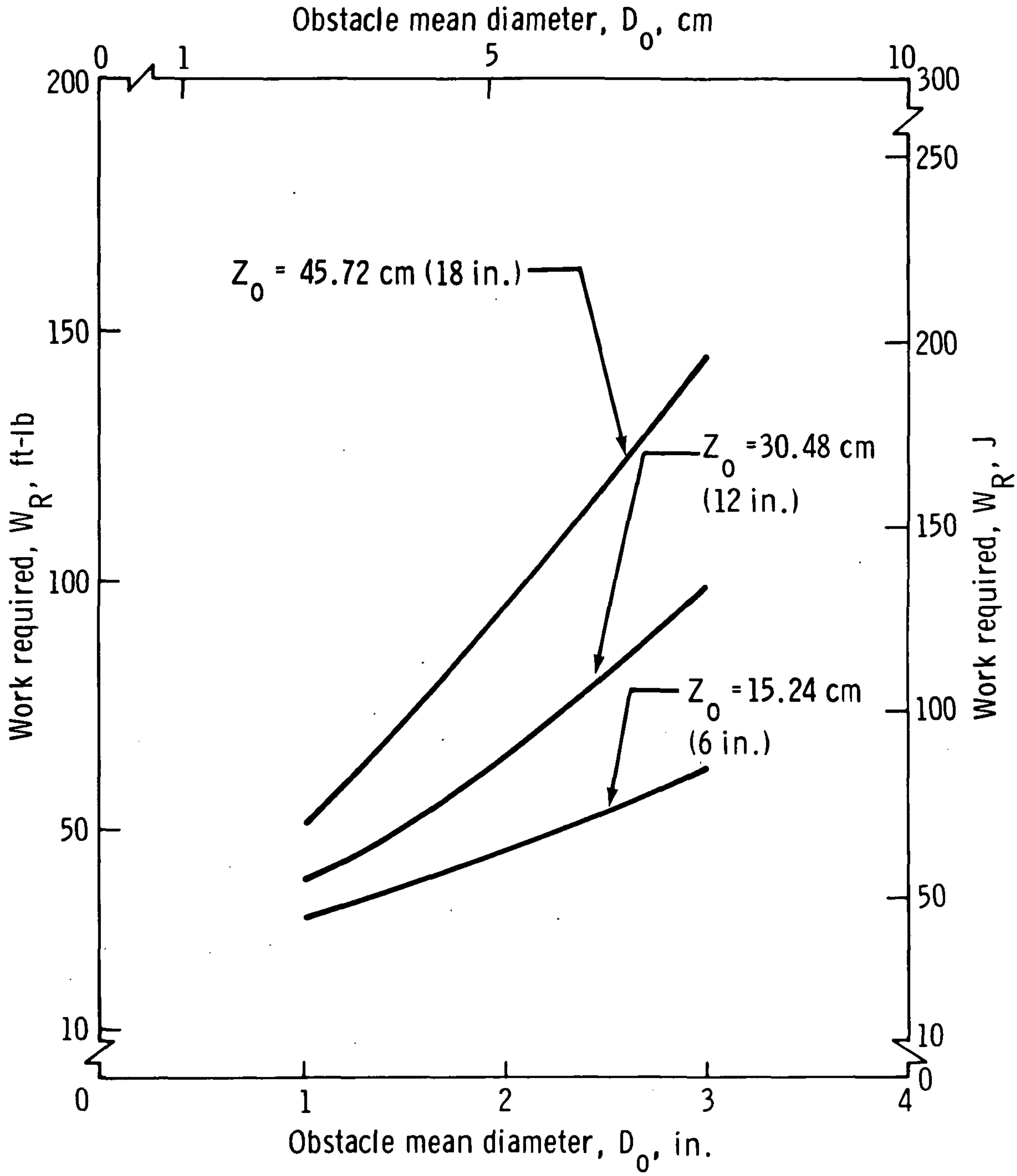

Figure 24. - Effects of obstacle size in Standard Ottawa Sand (D_r = 50 percent).

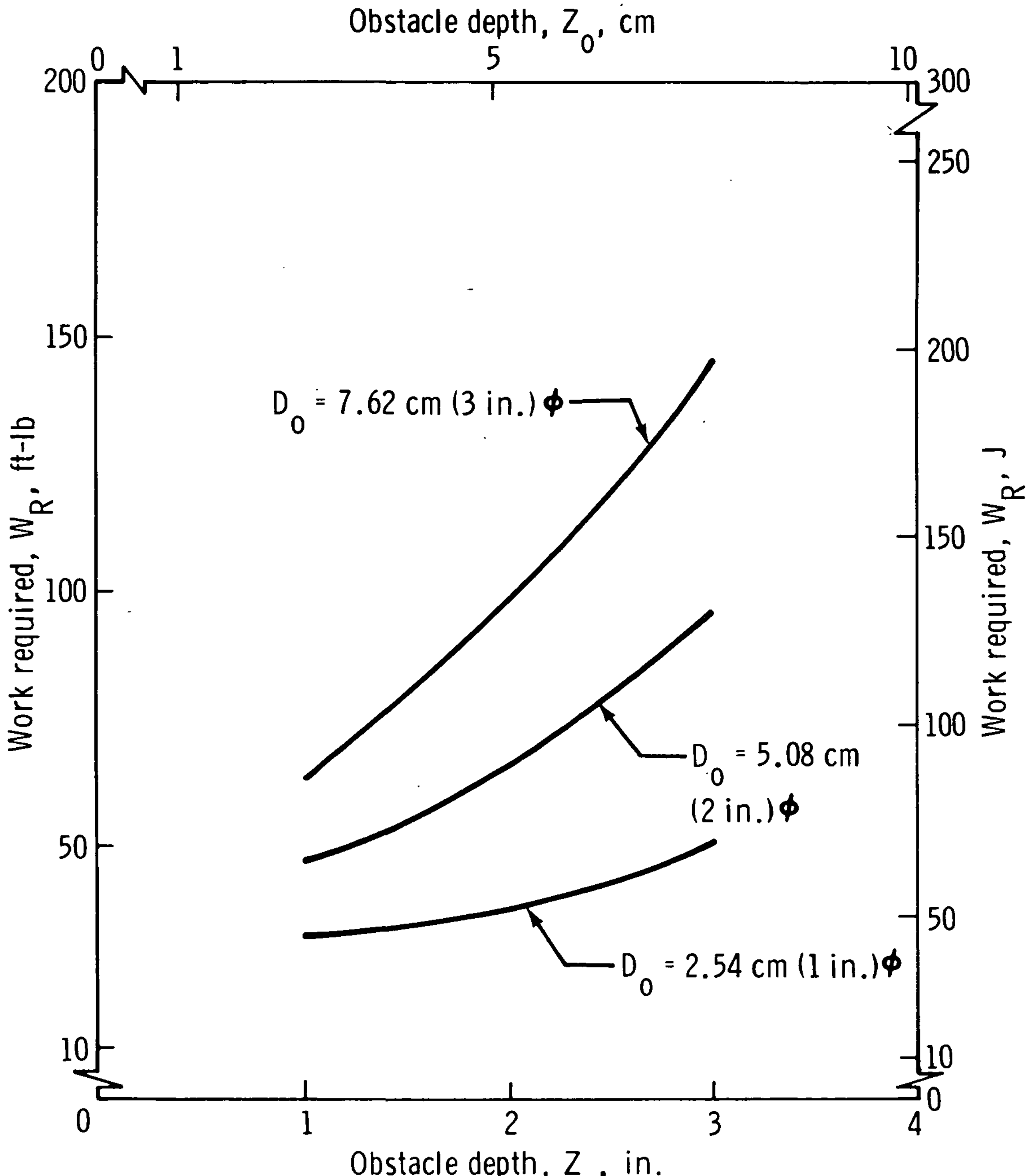

Figure 25. - Effects of obstacle depth in Standard Ottawa Sand (D_r = 50 percent).

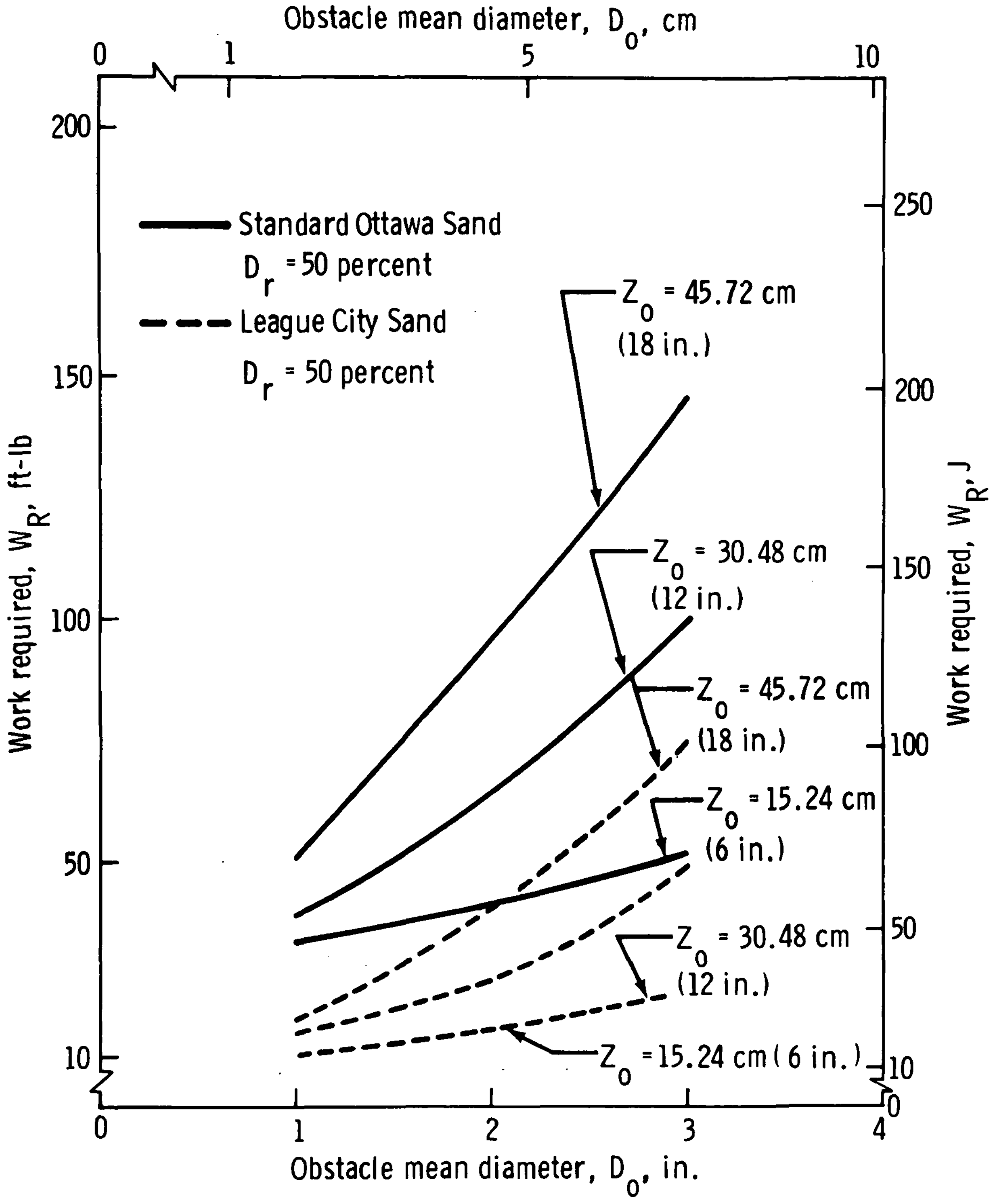

Figure 26. - Effects of average grain size.

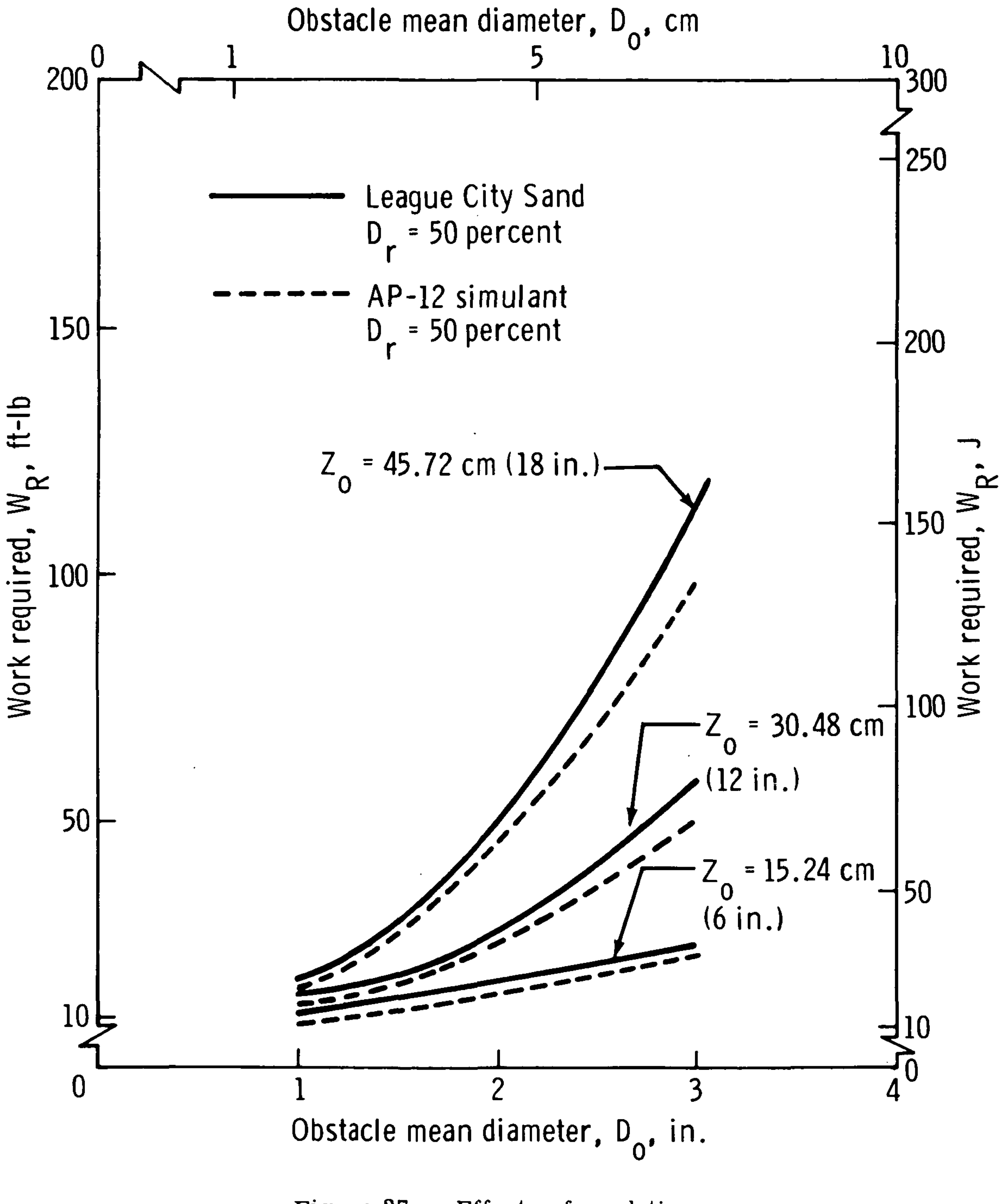

Figure 27. - Effects of gradation.

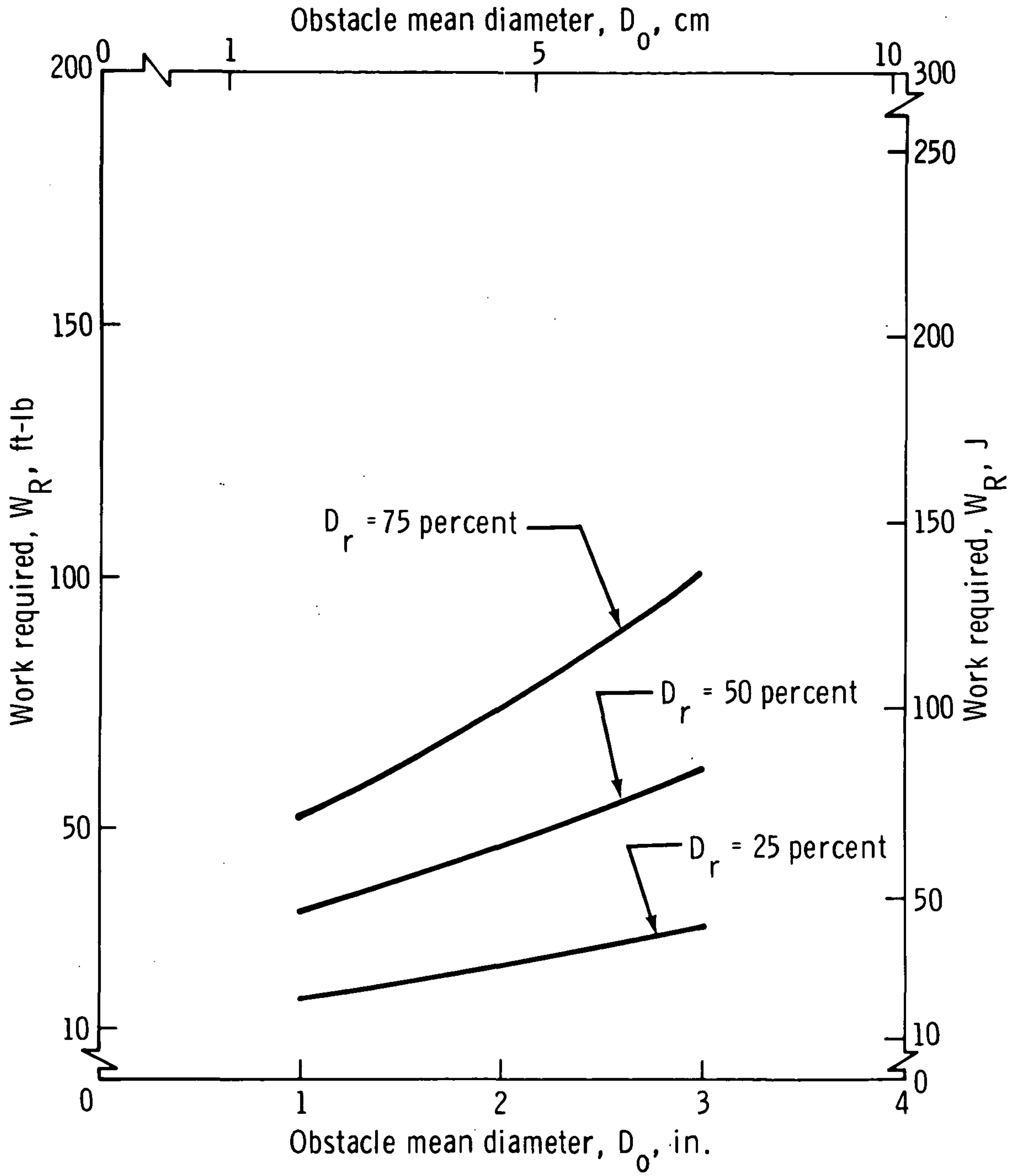

Figure 28. - Effects of relative density in Standard Ottawa Sand 15.24 cm (6 in.) deep.

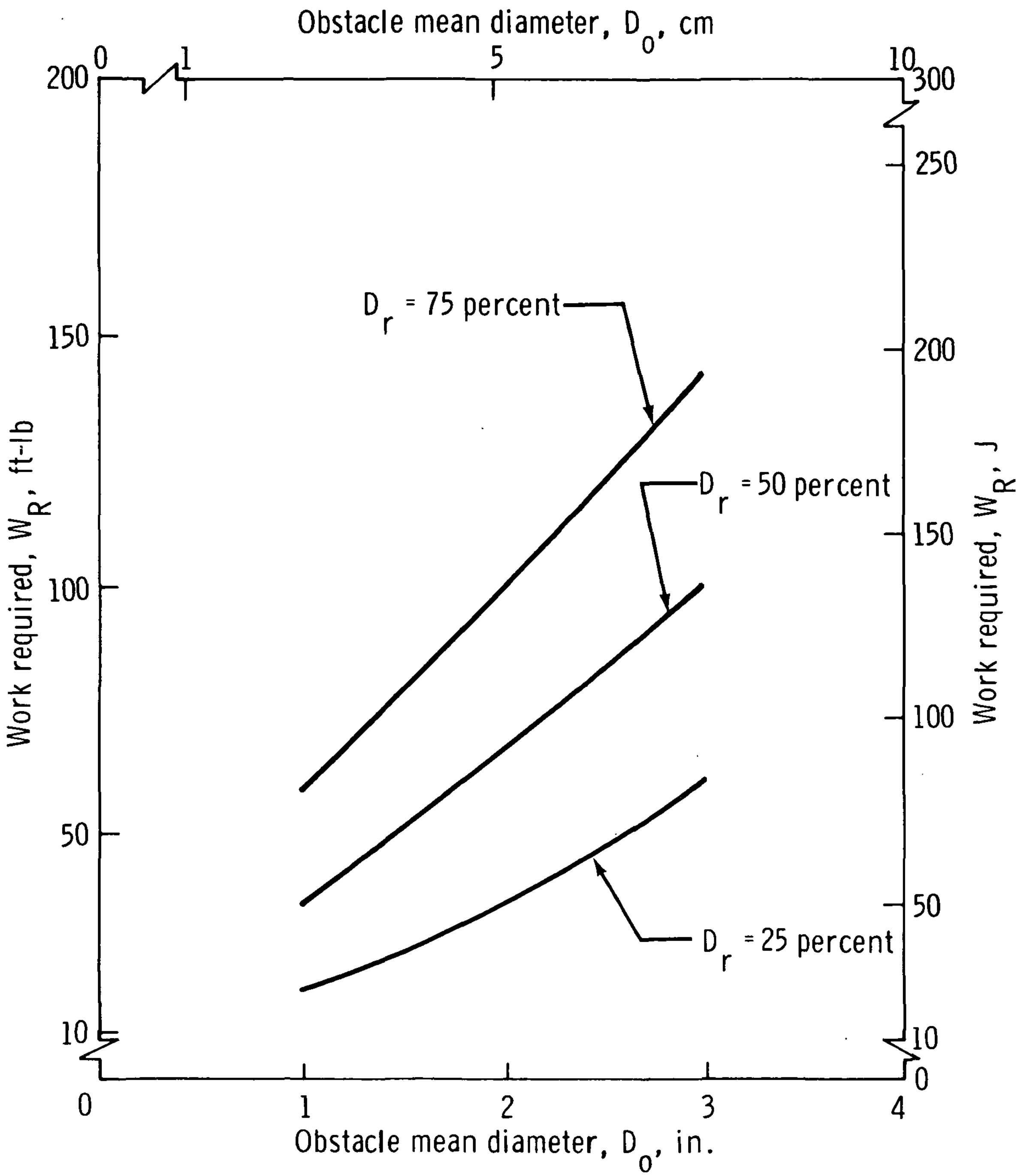

Figure 29. - Effects of relative density in Standard Ottawa Sand 30.48 cm (12 in.) deep.

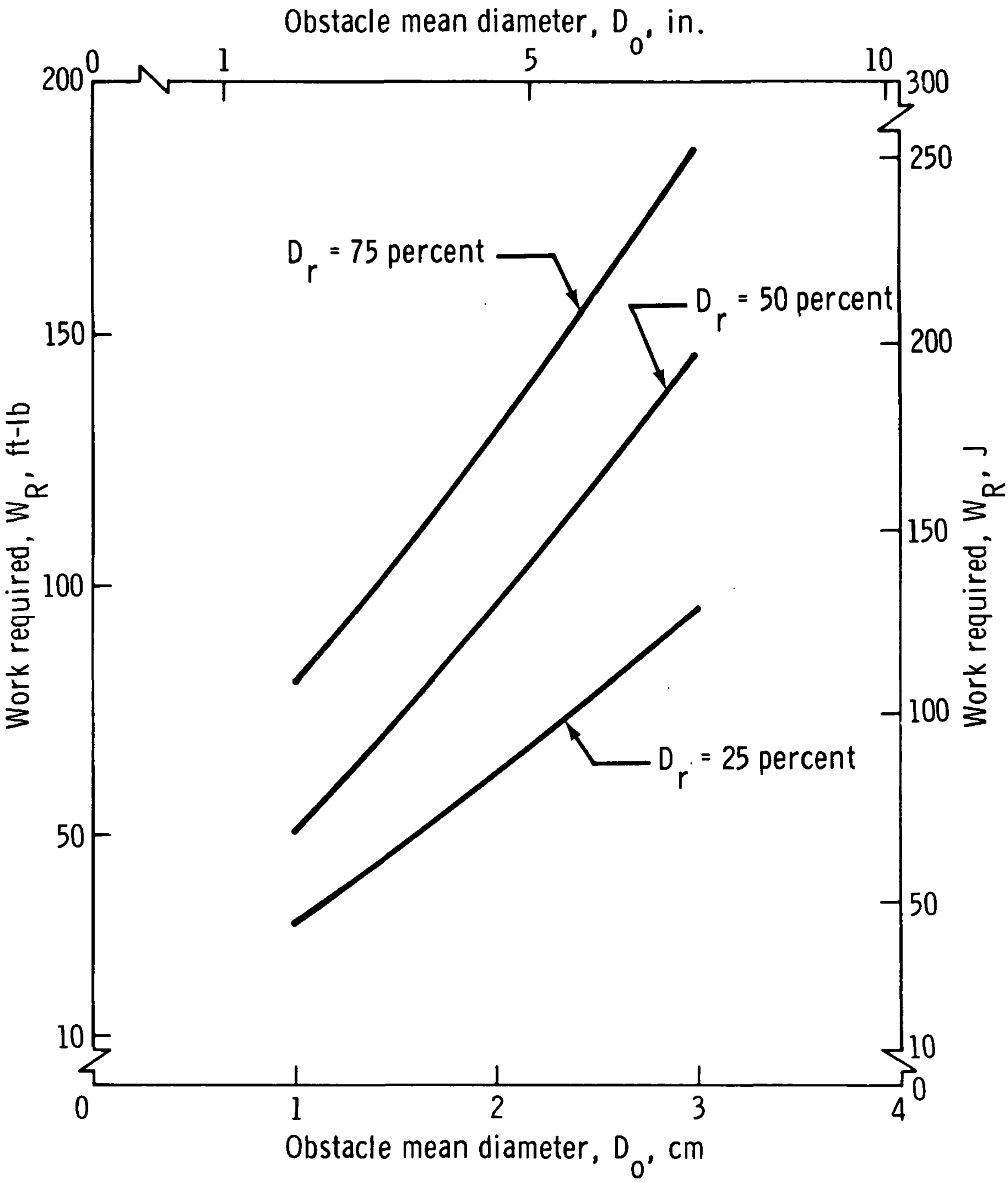

Figure 30. - Effects of relative density in Standard Ottawa Sand 45.72 cm (18 in.) deep.

APPENDIX A

GRAIN-SIZE-DISTRIBUTION CURVES

A laboratory grain-size analysis was performed on each soil specimen. Test data obtained from table A-I were used to plot the resulting distribution curves shown in figure A-1. The U.S. Bureau of Standards Sieve Series was used in the analyses, with the exception of AP-12, which required an additional hydrometer analysis for grain diameters less than 0.074 millimeter. The uniformity coefficient for each soil was computed from the following standard equation.

$$C_u = D_{60}/D_{10} \tag{A-1}$$

Values for these coefficients are summarized in table A-II.

A small value of C_u indicates uniformity with grain size, the ideal value being 1.00, while large values conversely indicate a wide range of grain sizes. Because for the first three soils analyzed $1.00 < C_u < 2.30 << 6.17$, these soils may be considered uniform, and the last (AP-12) may be considered well graded.

TABLE A-I. - GRAIN-SIZE DISTRIBUTION

Grain diameter, mm (in.)	Percent finer by weight			
	MS	OS	LCS	AP-12
4.760 (0.1874)	100.0	--	--	--
3.360 (.1323)	96.8	--	--	--
2.380 (.0947)	84.0	--	--	--
2.000 (.0787)	72.6	--	--	--
1.680 (.0661)	47.9	--	--	--
1.190 (.0469)	20.1	--	--	--
1.000 (.0394)	--	100.0	100.0	--
.840 (.0331)	6.4	97.9	98.5	--
.590 (.0232)	3.2	55.5	97.8	--
.420 (.0165)	--	5.8	96.0	--
.417 (.0164)	--	--	--	92.8
.297 (.0117)	--	.7	94.2	--
.250 (.0098)	--	--	92.4	84.9
.210 (.0083)	--	--	90.0	--
.177 (.0070)	--	.03	73.0	--
.149 (.0059)	--	--	56.8	75.2
.105 (.0041)	--	--	22.1	69.4
.074 (.0029)	--	--	7.9	63.2
.062 (.0024)	--	--	--	58.3
.058 (.0023)	--	--	--	50.9
.053 (.0021)	--	--	2.4	--
.042 (.0017)	--	--	--	44.9
.032 (.0013)	--	--	--	34.9
.023 (.0009)	--	--	--	24.3
.017 (.0007)	--	--	--	16.0
.013 (.0005)	--	--	--	11.3
.0091 (.0004)	--	--	--	7.1
.0065 (.0003)	--	--	--	3.5
.0053 (.0002)	--	--	--	2.4

TABLE A-II. - UNIFORMITY COEFFICIENTS

Soil type	Uniformity coefficient C_u
MS	2.30
OS	1.20
LCS	1.90
AP-12	6.17

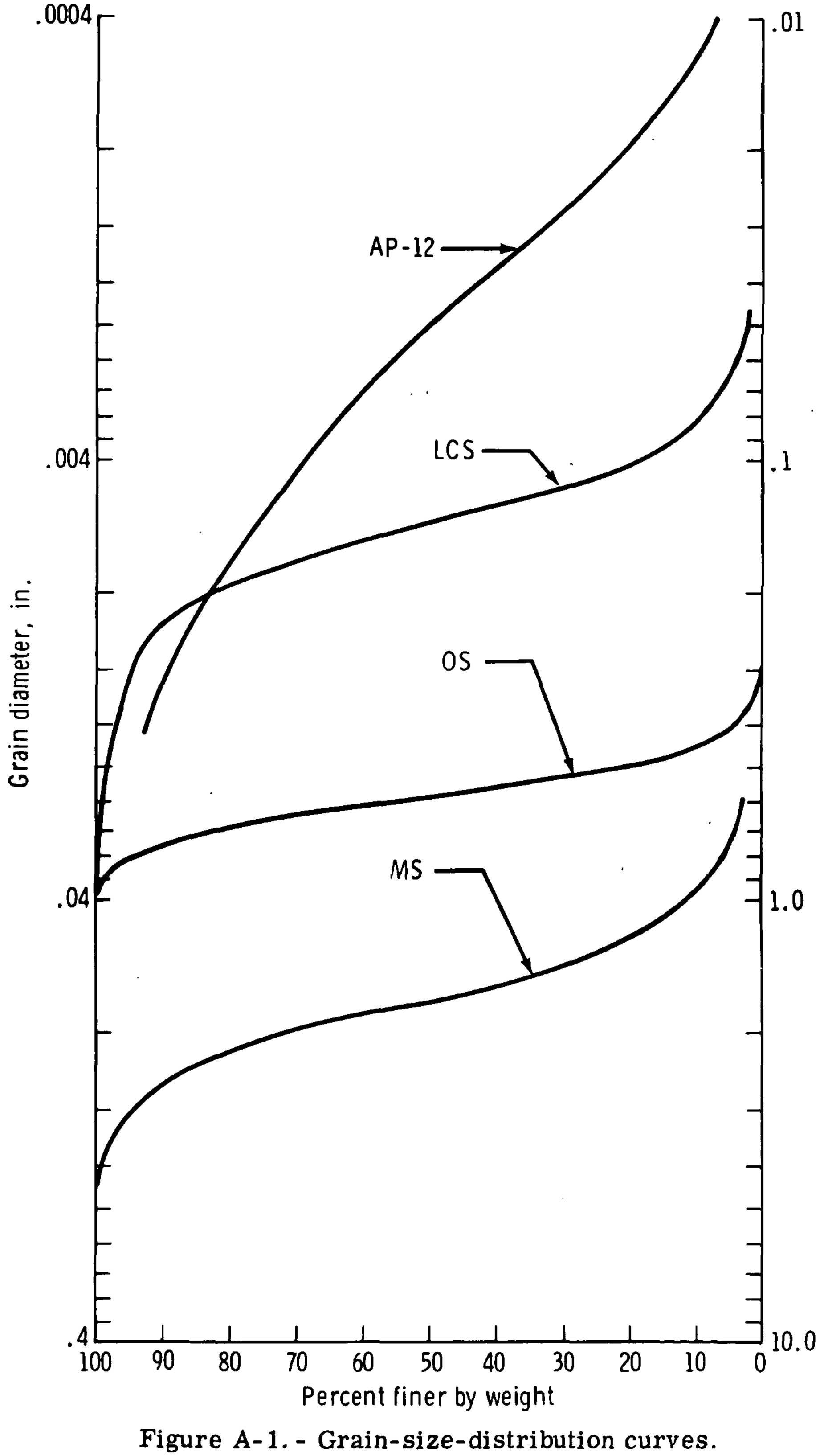

Figure A-1. - Grain-size-distribution curves.

APPENDIX B

STANDARD PENETRATION RESISTANCE CURVES

Penetration resistance in soils is a measure of applied vertical force and, for constant density, it varies somewhat linearly with depth. For a particular relative density, a standard penetration resistance profile is defined as the average force compared to depth curve established by a minimum of three penetrations. Profiles of the four soils investigated are found in figures B-1 to B-4. The range of relative densities considered for analysis are listed in table B-I. A photograph of the procedure and laboratory apparatus used to establish standard penetration curves is shown in figure C-4.

TABLE B-I. - RANGE OF RELATIVE DENSITIES

Soil type	Percent relative density, D_r				
MS	0	25	50	--	100
OS	0	25	50	75	100
LCS	--	25	50	75	100
AP-12	--	35	50	65	85

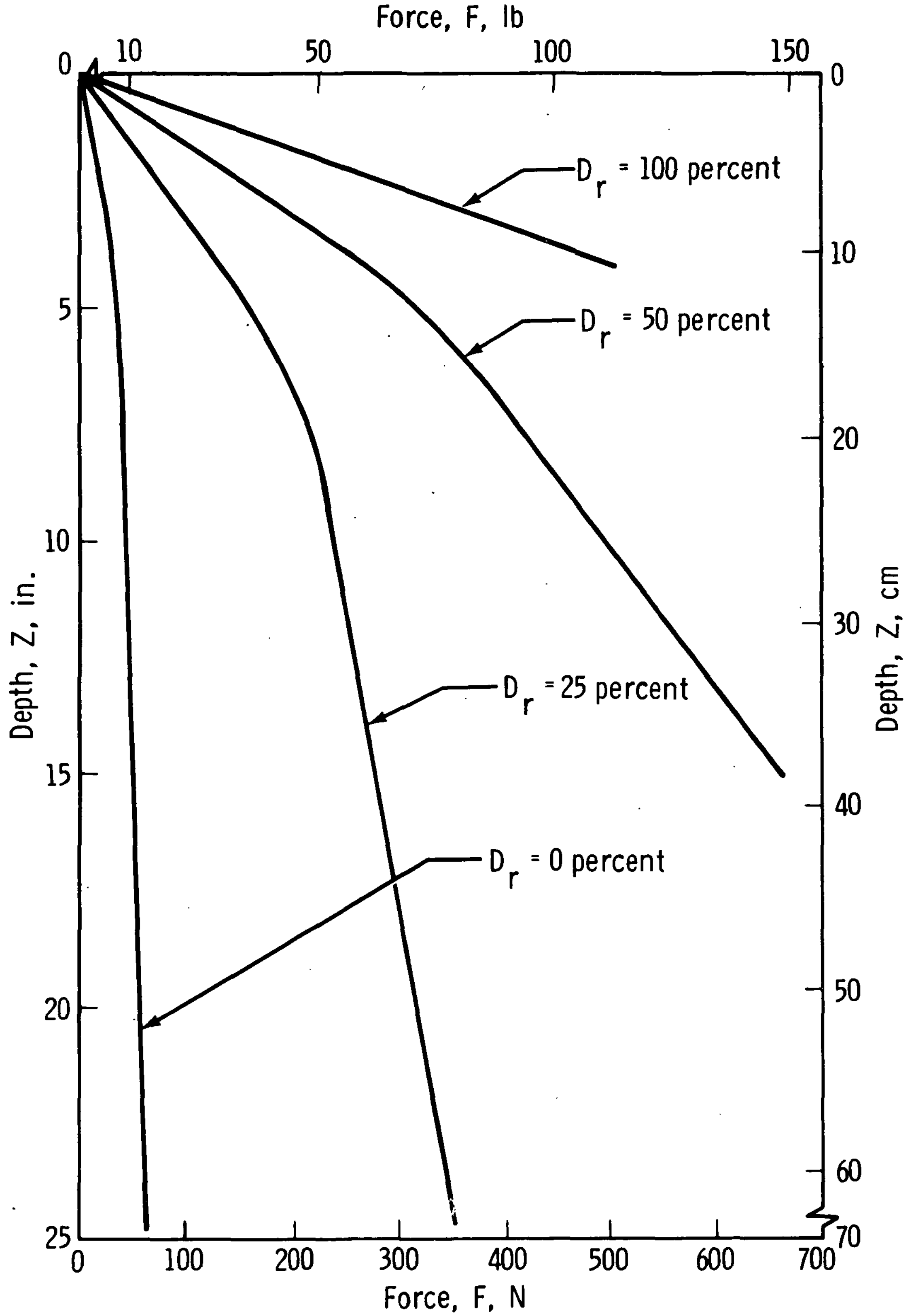

Figure B-1. - Standard penetration resistance curves for Bendix Medium Sand.

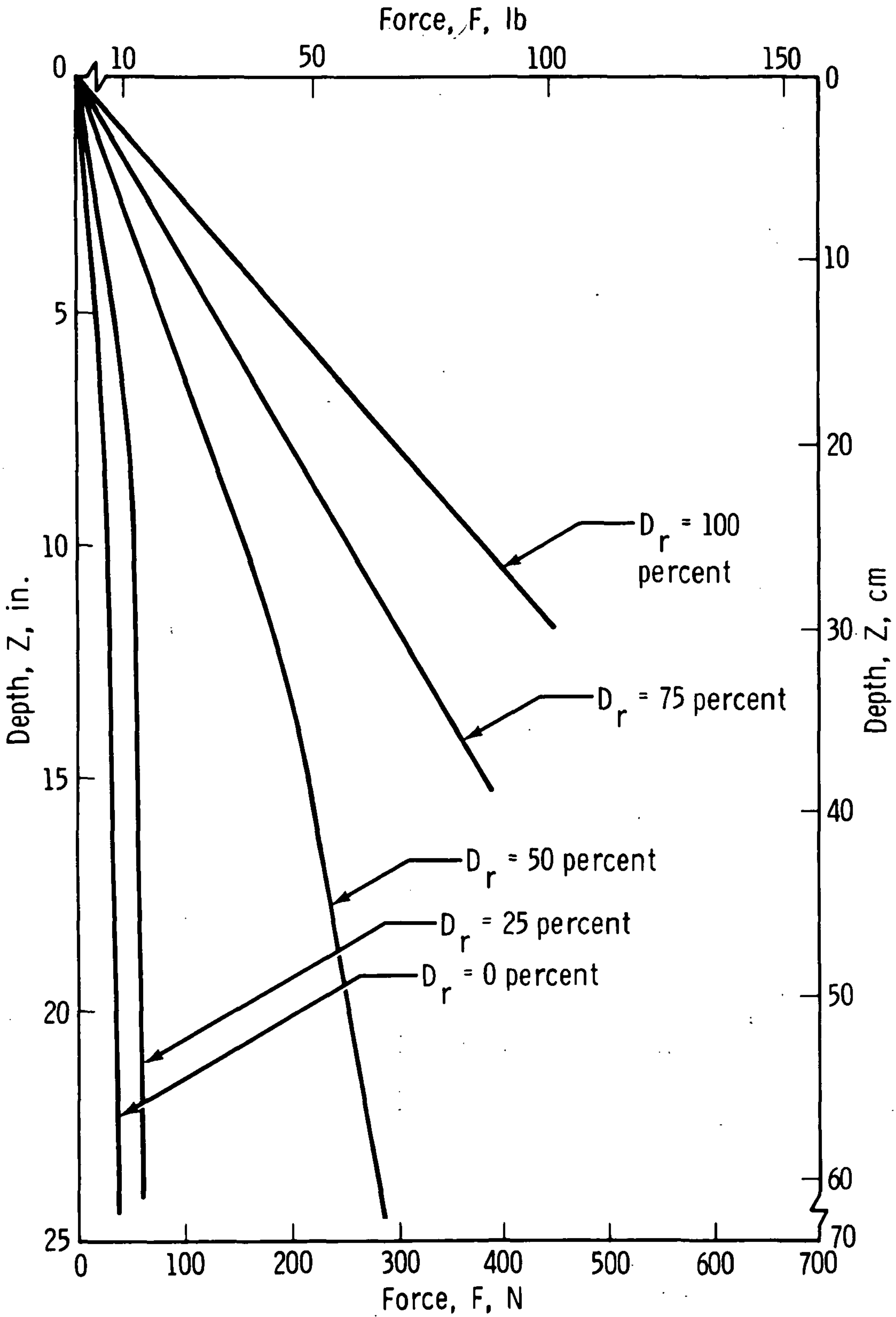

Figure B-2. - Standard penetration resistance curves for Standard Ottawa Sand.

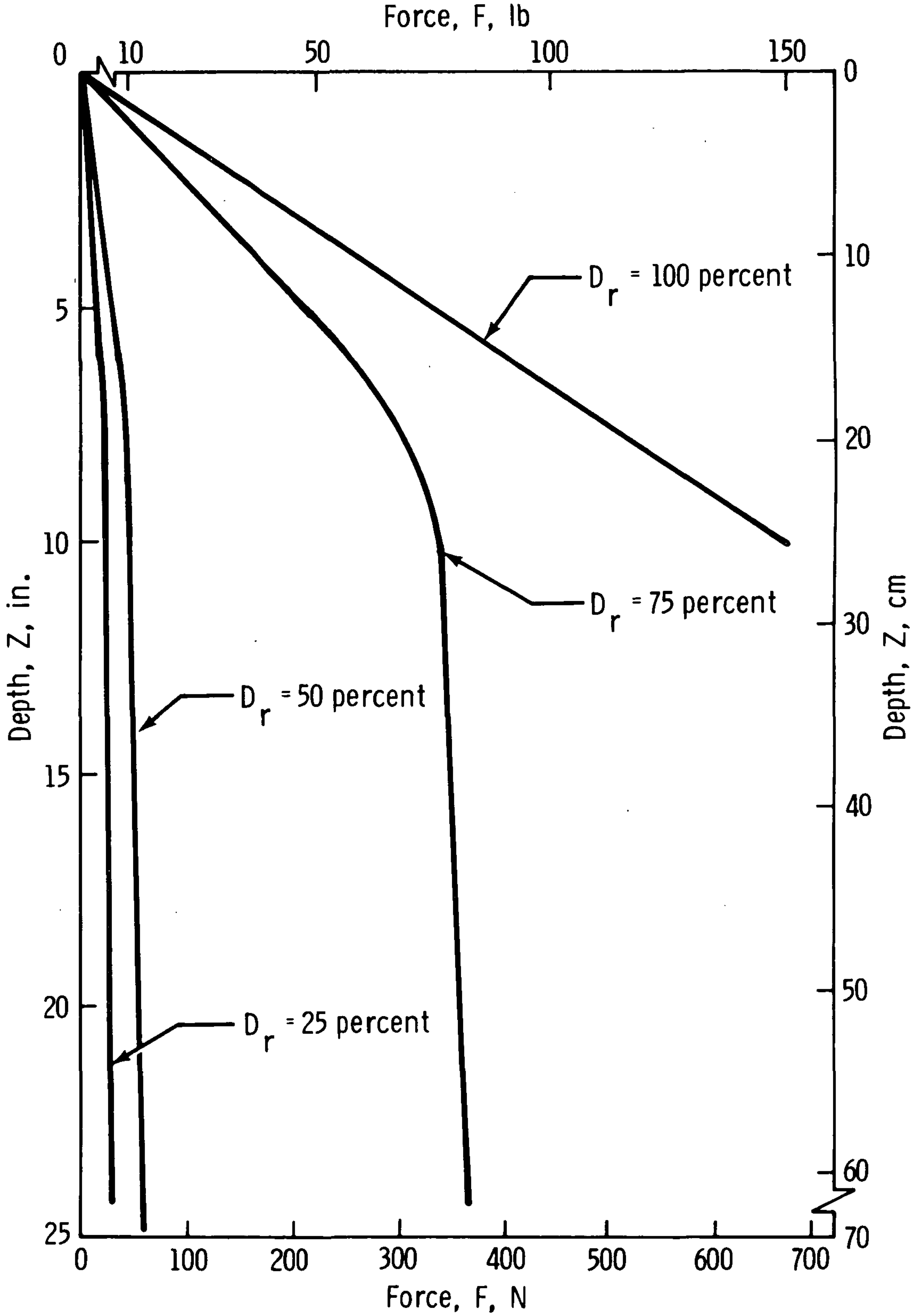

Figure B-3. - Standard penetration resistance curves for League City Sand.

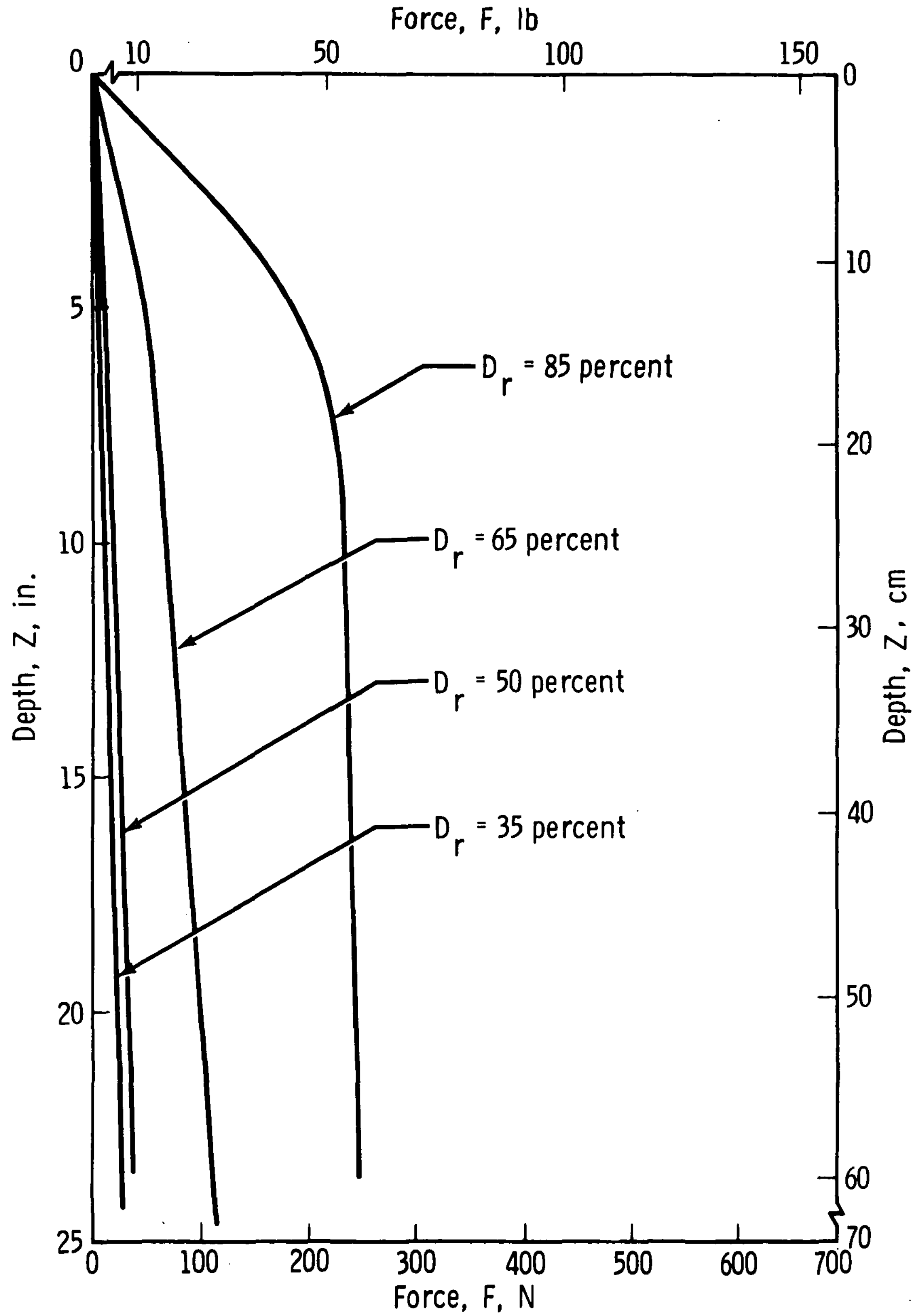

Figure B-4. - Standard penetration resistance curves for AP-12.

APPENDIX C

PHOTOGRAPHS

This appendix contains several photographs illustrating equipment and procedures utilized in establishing obstacle penetration profiles. The order of appearance, with a brief explanation accompanying each figure, is listed below.

Figure C-1

The head of the penetrometer unit consists of a standard WES 30° cone with a 6.35 cm (2.50-inch) shank. Both shank and cone are made of heat-treated carbon steel. The shank contains the load cell transducer used to record resistance.

Figure C-2

The handle consists of a removable, slightly convex hand plate and shank (collar). The shank contains a receptacle (jack) for the load cell power input. The stem is a hollow 1.57 cm (5/8-inch) ϕshaft containing wiring for the load cell power input and load cell transducer. Both stem and handle are manufactured from lightweight aluminum.

Figure C-3

The mold adopted as the standard for obstacle penetration studies consists of a hollow steel cylinder and base plate and has a total weight of 108.2 kilograms (238.5 pounds). For mold dimensions, see figure 3.

Figure C-4

The equipment used for a typical obstacle penetration study includes the following.

1. Standard mold and template cover (lower right)
2. Standard penetrometer with WES 30° cone (middle right)
3. Depth cell mounted on hoist boom (upper right)
4. Data acquisition system (left) and power input (center)

The typical experimental procedure includes the following.

1. Timing and rate of penetration (left)
2. Application of an even rate of penetration (right)

Equipment and procedures used to establish standard penetration profiles are similar to those just listed.

Figure C-5

The data acquisition system is capable of controlling 43 separate input-output channels. Only the first three were utilized in this study, as shown below.

1. Channel 0, load cell output

2. Channel 1, load cell power input

3. Channel 2, depth cell output

Instantaneous readings of time (lower left), channel selection (center), and channel voltage (top) were recorded on paper tape (lower right).

Figures C-6 Through C-9

In figure C-6, obstacles are positioned in the standard mold for penetration study, showing relative location and size. This particular depth is 30.48 cm (12 inches). In figures C-7, C-8, and C-9, effects of penetration on obstacles are shown. Black arrows indicate "strike lines" of the penetrometer cone.

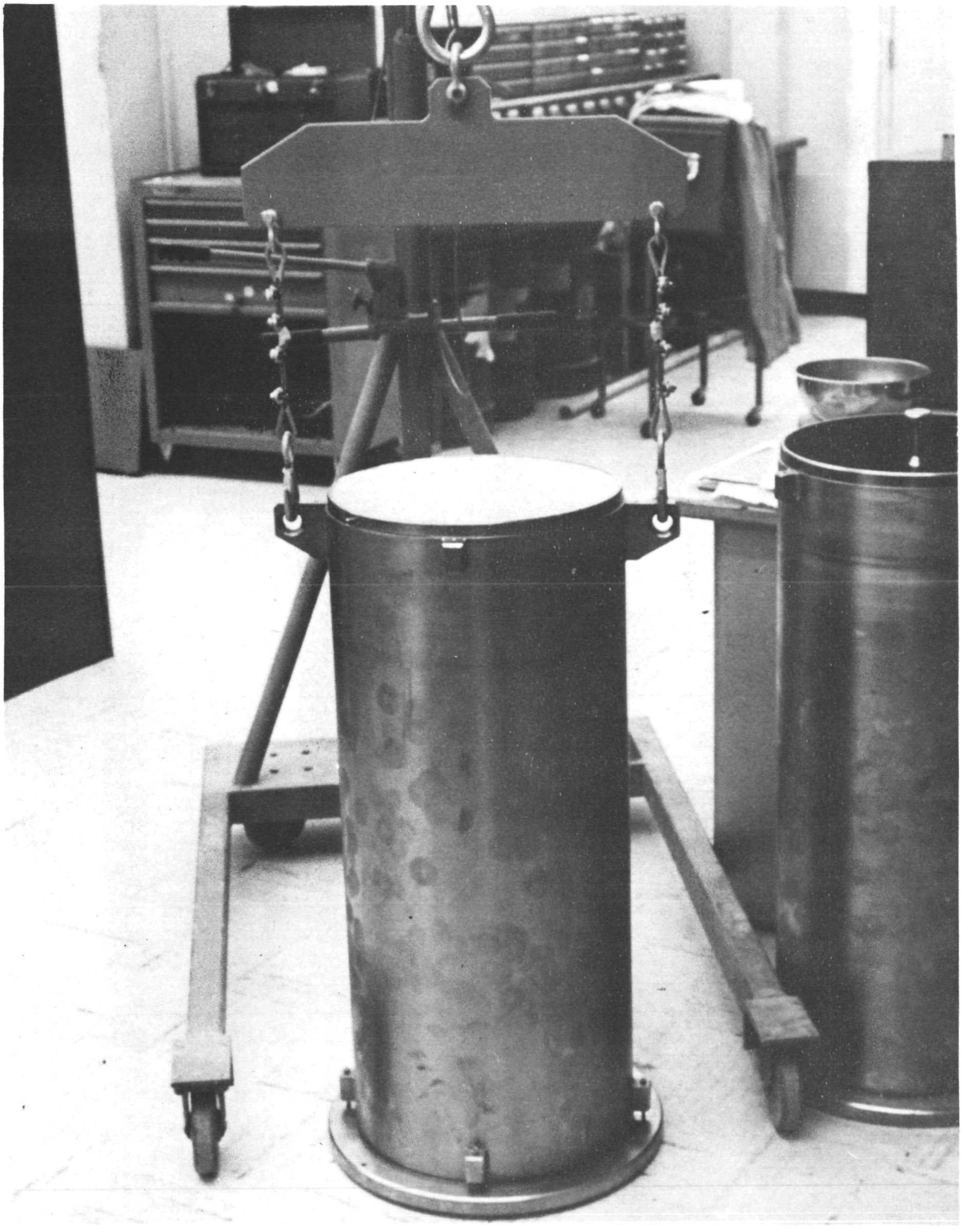

Figure C-3. - Standard mold.

Figure C-4. - Obstacle penetration study.

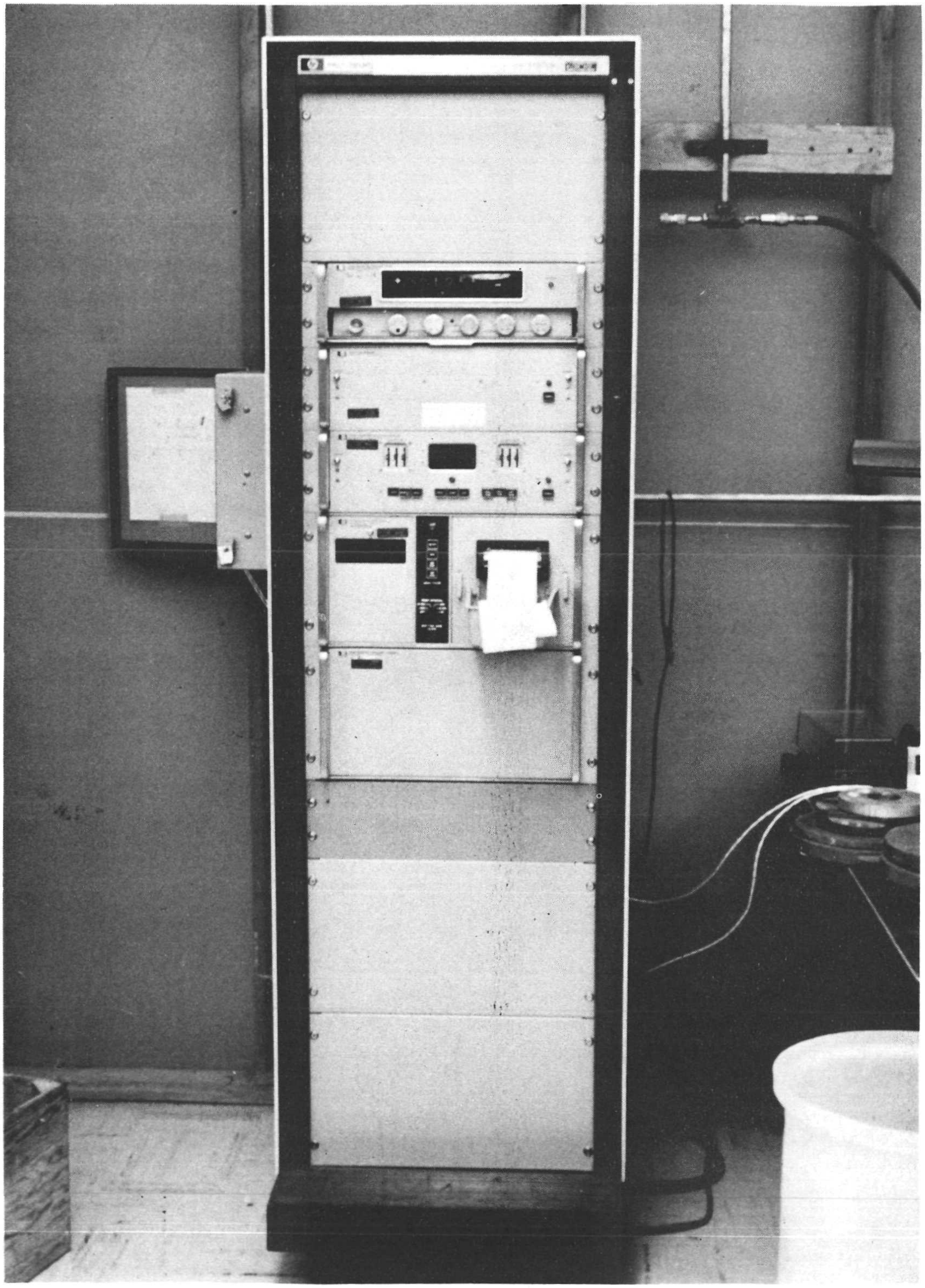

Figure C-5. - Data recording unit.

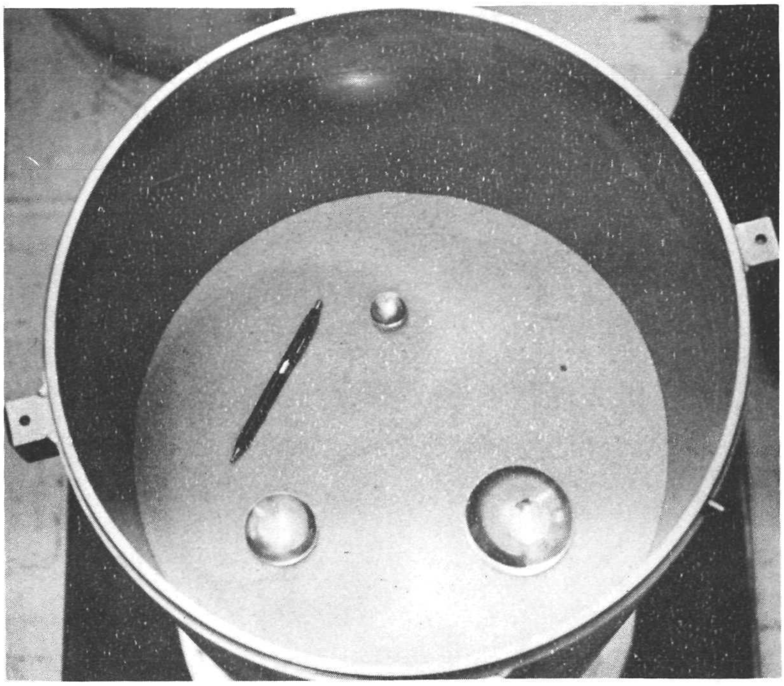

Figure C-6. - Obstacles positioned in the standard mold.

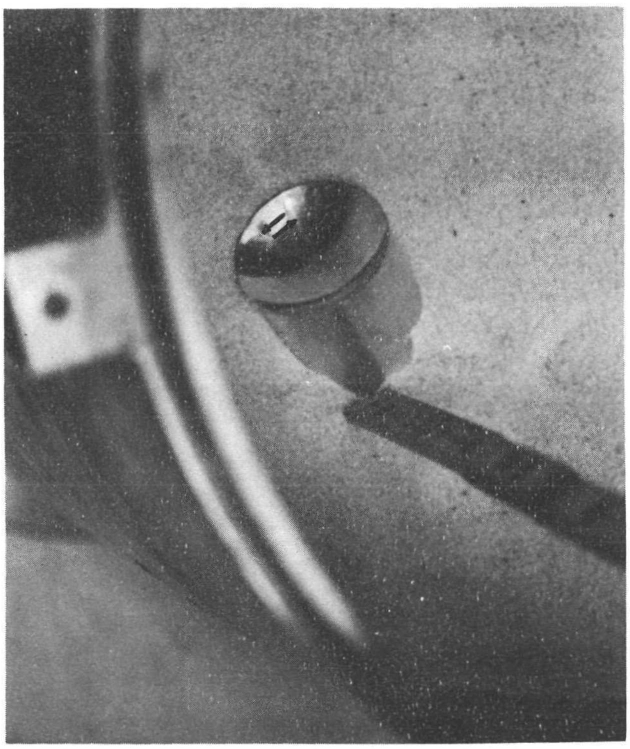

Figure C-7. - Effect of penetration on obstacle, view 1.

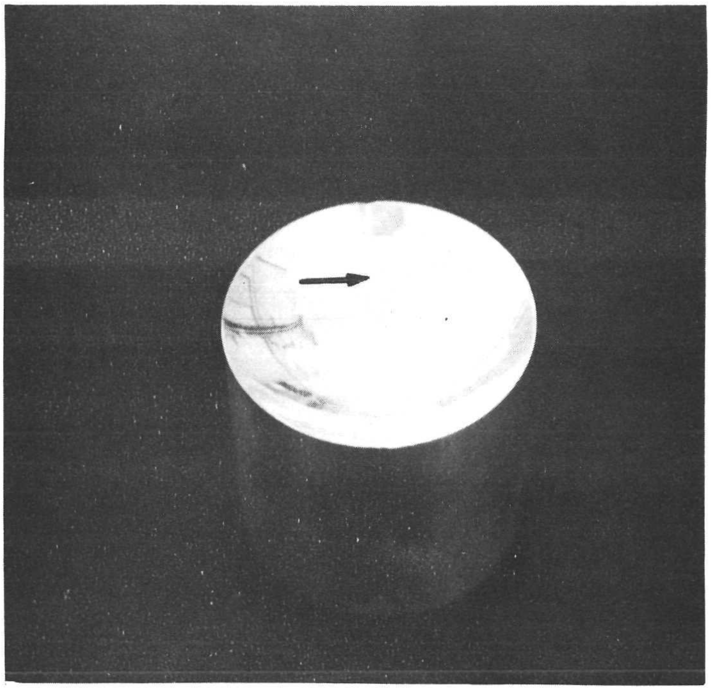

Figure C-8. - Effect of penetration on obstacle, view 2.

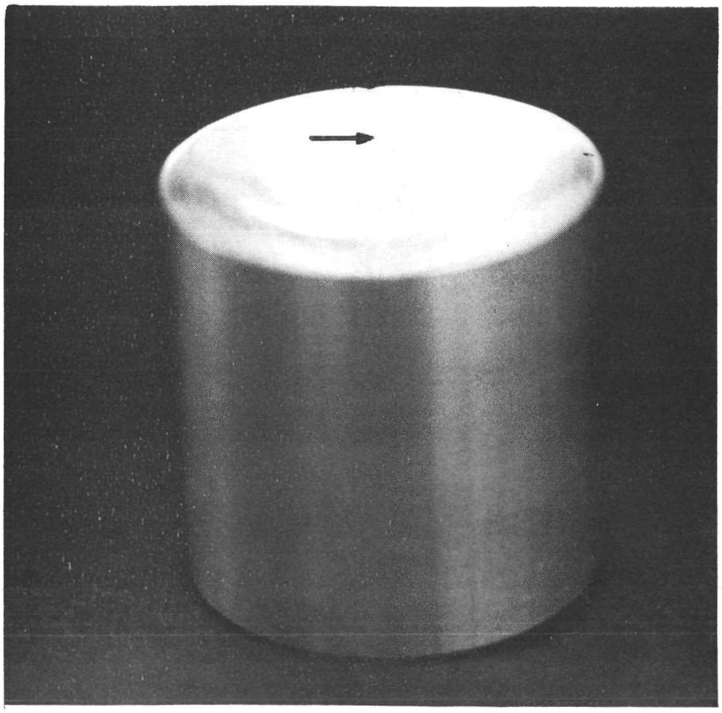

Figure C-9. - Effect of penetration on obstacle, view 3.

NASA — MSC